Deanship of Graduate Studies
Al-Quds University

Elucidating the molecular interactions of human immunoglobulins with liposomal drug carriers

Nancy Hazem Mohammad Mohammad

M.Sc. Thesis

Jerusalem - Palestine

1444 / 2023

Elucidating the molecular interactions of human immunoglobulins with liposomal drug carriers

Master thesis by: Nancy Hazem Mohammad Mohammad

1st Supervisor: Dr. Sawsan Abusharkh

2nd Supervisor: Dr. Agnes Csiszár

The present thesis was performed in collaboration between Al-Quds University and Forschungszentrum Jülich GmbH, Germany. The experiments were conducted in the Institute of Biological Information Processing: Mechanobiology (IBI-2) within the Forschungszentrum Jülich GmbH between October 10, 2021 and April 10, 2022. The thesis was supervised by Dr. Agnes Csiszár from IBI-2 and Dr. Sawsan Abu Sharkh from Al-Quds University.

As Partial Fulfillment of the Requirements for the Degree of Master of Science in Physics, this thesis was submitted to the Faculty of Science and Technology, Al-Quds University.

1444 / 2023

Al-Quds University
Deanship of Graduate Studies
Physics Department

Thesis Approval

Elucidating the molecular interactions of human immunoglobulins with liposomal drug carriers

Prepared by: Nancy Hazem Mohammad Mohammad

Registration No.: 21812405

Supervisor: Dr. Sawsan Eid Hamed Abusharkh

Master thesis submitted and accepted, Date: 5 / 4 / 2023

The names and signatures of the examining committee members are as follows:

1. **Head of Committee: Dr. Sawsan Abusharkh Signature** ……
2. **Internal Examiner: Dr. Hussein Hallak Signature** ……
3. **External Examiner: Dr. Mohmmad Qneibi Signature.** ……

Jerusalem

1444 / 2023

Dedication

I dedicate this work to my lovely family and my husband who always encourages me with passion and endless support. To my faithful friends; Afrah, Eklas, Heba, Wala, Aya, Ghadeer, Dema, Kouther, Rama, and Ondra, who have always supported me and believed in me…

To My Supervisors Dr. Agnes Csiszár and Dr. Sawsan Abusharkh who spare no effort for this research to succeed.

Nancy Mohammad

Declaration

I certify that this thesis submitted for the degree of master, is the result of my own research, except where otherwise acknowledged, and that this thesis (or any part of the same) has not been submitted for a higher degree to any other university or institution.

Signed: nancy mohammad

Nancy Hazem Mohammad Mohammad

Date: 23 / 5 / 2023

Acknowledgments

Firstly, I would like to thank Prof. Rudolf Merkel for allowing me to work at his institute, for his availability for discussions of results, which has been incredibly helpful and motivating.

I am especially grateful to my supervisors, Dr. Agnes Csiszar, for her guidance during the experimental process. Thanks for your time and for teaching me many things in laboratory, for countless discussions, for your patience, and for providing assistance when I arrived in Jülich.

For my Palestinian supervisor Dr. Sawsan Abusharkh, thank you for giving me the opportunity to go to Germany, which was an amazing experience from which I learned a great deal, as well as her knowledge and valuable advice.

Throughout my time at the IBI2 and at Al-Quds University, I am thankful to all my colleagues who offered help whenever I needed it.

Abstract

Nanocarriers' success in biomedical applications depends largely on their uptake efficiency. In most cases biomolecules like proteins, DNA, and antibiotics are taken up via endocytosis by living cells. These cell organelles are part of the cell's catabolic system, thus leading to enzymatic degradation of the NPs. A more promising alternative is to induce membrane fusion between the carrier and the cellular membrane for efficient molecular delivery. Therefore, liposomes with highly fusogenic prosperities have been developed at the Research Center of Jülich, called fusogenic liposomes (FLs) [1]. Applications relying on FLs as molecular delivery purposes have been successfully applied i.e. proteins, anti-cancer drugs, DNA, mRNA and siRNA [1] [2], but the exact mechanism of fusion has to be elucidated in more detail in future analysis.

If nanoparticles are injected into the blood stream, they interact with hundreds of biomolecules that adsorb on their surface forming the so-called "protein corona". Immunoglobulin G (IgG) is a corona-forming protein, mainly involved in immune reactions. IgG behaves as opsonin, which decrease the circulation time, promote inflammation, allergic reactions, and increase blood clearance by inducing complement activation [3]. Nevertheless, the mechanism underlying immunoglobulin-nanoparticles interaction is yet unspecified.

Therefore, this work has aimed to investigate the interaction of IgG with different liposomal formulations including fusogenic liposomes (FL), PEGylated liposomes (DOPC-PEG), and neutral liposomes (DOPC) as a control.

For characterization of the liposomes/IgG complexes, dynamic and electrophoretic light scattering (DLS and ELS), respectively were applied. The stability and IgG affinity to different liposomal formulations were investigated by fluorescence quenching spectroscopy and isothermal titration calorimetry (ITC). Stern and modified Stern-Volumer equations and ITC plots were used to calculate binding constants, binding site, and thermodynamics parameters of IgG/liposomes complexes.

The results of DLS and ELS showed that IgG adsorbed only on FL surfaces, as indicated by a significant increase in hydrodynamic diameter and a neutral zeta potential values approaching

that of free IgG. Furthermore, PEGylated liposomes prevent IgG adsorption due to their low PEG density used (5%). Observations of fluorescence spectroscopy show that the structural change in IgG remains stable, but the quenching effect was only observed in FL. Further analysis of fluorescence data show that the FL/IgG complexes are electrostatically bound. Meanwhile, ITC shows mainly hydrophobic forces govern the FL/IgG complex. No binding was observed, with neutral liposomes (DOPC). While DOPC-PEG shows a contradictory result that indicates non-covalent binding with IgG. Further research may provide more accurate results. The results of this study suggest that FLs could be a promising safe therapeutic carrier in drug delivery.

.

دراسة التفاعلات الجزيئية بين البروتين المناعي (IgGs) مع الجسيمات النانوية

اسم الطالبة: نانسي حازم محمد محمد.
اسم المشرف: الدكتورة سوسن عيد أبو شرخ.

الملخص

يعتمد نجاح الجسيمات النانوية في التطبيقات الطبية الحيوية إلى حد كبير على قدرتها على الاندماج بكفاءة مع الخلايا الحية وتفادي الجهاز المناعي. ولكن في معظم الحالات، تقوم الخلايا بامتصاص الجزيئات عبر عملية تدعى الالتقام الخلوي"endocytic pathway"، حيث تعمل على إدخال جزيئات مثل البروتينات والحمض النووي والمضادات الحيوية إلى الخلايا الحية. من سلبيات هذه العملية أنها تحارب الجسميات النانوية "جسم غريب" مما يؤدي إلى إفراغ محتوياتها وبالتالي تدميرها عبر الجسيمات الحالة. أظهرت العديد من الدراسات أن تحفيز اندماج الغشاء بين المادة الحاملة " الجسيمات النانوية " والغشاء الخلوي في الداخل يؤدي إلى توصيل جزيئي فعال. لذلك، تم تطوير جسيمات نانوية لها قدرة عالية على الاندماج مع الغشاء الخلوي، في مركز الأبحاث في يوليش ، حيث اطلقوا عليها اسم (Fusogenic liposomes 'FL') [4] .تم اختبار قدرة هذه الجسيمات FLs على إيصال جزيئات مثل البروتينات والعقاقير المضادة للسرطان والحمض النووي و mRNA و siRNA [2] [1]، حيث اظهرت قدرة عالية على الاندماج وايصال الجزيئات بشكل آمن وفعال، ولكن يجب توضيح الآلية الدقيقة للاندماج بمزيد من التفصيل في الأبحاث المستقبلية.

يتم حقن الجسيمات النانوية في مجرى الدم حيث تتفاعل مع مئات الجسيمات الموجودة بالدم، مما يؤدي إلى التصاق بعض هذه الجسيمات على سطحها مكونة ما يسمى بـ الهالة البروتينية "Protein corona". قد تحتوي هذه الهالة البروتينية على جسيمات من الجهاز المناعي، مثل الغلوبولين المناعي (IgGs) حيث يمثل جزء رئيسي في الدم، ويشارك في تفعيل جهاز المناعة [3]. ومع ذلك، فإن الآلية الكامنة وراء تفاعل IgGs مع الجسيمات النانوية بحاجة لمزيد من التفصيل.

لذلك، يهدف هذا العمل إلى دراسة الاستجابة المناعية للغلوبولين المناعي IgG تجاه جسيمات نانوية مختلفة تشمل: جسيمات اندماجية (FL) ، و جسيمات نانوية مرتبطة ببوليمر (DOPC-PEG)، وجسيمات تحمل شحنة متعادلة (DOPC) لتستخدم كمرجع.

تم استخدام العديد من التقنيات لدراسة التفاعل بين IgG والجسيمات النانوية المختلفة ، مثل: Dynamic and Electrophoretic light scattering (DLS) and (ELS), fluorescence quenching spectroscopy and Isothermal titration calorimetry (ITC).

كما تم توظيف بعض المعادلات مثل Stern and modified Stern-volumer equations لحساب معامل الارتباط، وعدد مواقع الارتباط على IgG، والثوابت المرتبطة بالديناميكا الحرارية التي تحمل معلومات عن التفاعل.

أظهرت نتائج DLS وELS وجود ل IgG على سطح FL وقد تمثل ذلك في زيادة في قطر الجسيم FL و اكتسابه شحنة سالبة ناتجة عن وجود البروتين IgG الذي يحمل شحنة سالبة على سطح FL. أما الجسيمات المرتبطة ببوليمر " PEGylated liposomes" فقد عمل البوليمر على منع وصول البروتين IgG إلى سطحه، وذلك بسبب إضافة نسبة قليلة من البوليمر(PEG 5%) إلى الجسيم "DOPC-PEG ".

أظهرت نتائج المطيافية" fluorescence spectroscopy" ان البروتين IgG ارتبط فقط مع FL وأن عملية الارتباط FL / IgG لم تشمل تغيرا في البروتين IgG ولا في الطول الموجي للطيف الإنبعاثي للبروتين، حيث ان IgG ارتبط عن طريق القوى الالكتروستاتيكية مع FL. كما أكدت نتائج ITC هذا، اما الجسيمات المتعادلة فلم تظهر تفاعلا مع IgG بينما أظهرت نتائج الITC للجسيمات المرتبطة ببوليمر "DOPC-PEG " ان هناك تفاعل بينها وبين IgG مما يؤدي إلى تناقض مع النتائج السابقة خلال هذه الدراسة التي أظهرت عدم وجود تفاعل بينهم. لذا نحن بحاجة لإجراء مزيد من التجارب المستقبلية للجسيمات المرتبطة ببوليمر "DOPC-PEG" للحصول على نتائج دقيقة. أما بالنسبة للجسيمات الاندماجية FL فقد أظهرت نتائج هذه الدراسة إلى أن FLs يمكن أن يكون ناقلًا علاجيًا آمنًا واعدًا في توصيل الأدوية.

Contents

List of Tables

List of Figures

Acronyms

Complements components	**Comp.**
1,1'-Dioctadecyl 3,3,3',3- Tetramethylindotricarbocyanine Iodide	**DiR**
Differential scanning calorimetry	**DSC**
1,2-Dioleoyl-glycero-3-phosphocholine	**DOPC**
1,2-dioleoyl-sn-glycero-3-phosphoethanolamine	**DOPE**
1,2-dioleoyl-sn-glycero-3-phosphoethanolamine - N-[amino(polyethylene glycol)-2000]	**DOPE-PEG**
1,2-dioleoyl-3-trimethylammonium-propane	**DOTAP**
1,2-dioleoyl-3-N,N,N-trimethylaminepropane chloride	**DOTMA**
Enzyme linked immunosorbent assay	**ELISA**
Fourier transform infrared	**FTIR**
Fibrinogen	**Fg**
Fusogenic liposomes	**FLs**
Fragment antigen fab	**Fab**
Fragment crystalline	**Fc**
Giant unilamellar vesicles	**GUV**
Globins	**Glob.**
4-(2-hydroxyethyl)-1-piperazineethane-sulfonic acid	**HEPES**
Human Plasma	**HP**
Immunoglobulin G	**IgG**
Isothermal titration calorimetry	**ITC**
Nanoparticles	**NPs**
Phosphate buffer Saline	**PBS**
Photon correlation spectroscopy	**PCS**
Protein binding value	**PB**
Protein Corona	**PC**

Polyethylene glycol	**PEG**
Quasi elastic light scattering	**QELS**
Relative protein abundance	**RPA**
Reticuloendothelial system	**RES**
Room Temperature	**RT**
Small unilamellar vesicles	**SUV**
Tryptophan	**Trp**
Tryptophan residues	**Trps**
Transthyretin	**Ttr**
Trypsin	**TRY**
Trypsin inhibitors	**Tryp. inh.**
Large unilamellar vesicles	**LUV**
United State and food administration	**US FDA**
Vitronectin	**Vtn**

Chapter 1: Introduction

1.1 Problem Statement

The discovery of liposomes as drug carriers called the attention of scientists and industry. Liposomes are widely used due to their low toxicity, lack of immunogenicity, and biodegradability. Such liposomes demonstrate a preference for endocytosis uptake rather than fusion uptake; however, induced membrane fusion between liposomes and mammal's cell is a more promising approach for efficient molecular delivery [5]–[7]. Furthermore, molecular delivery by fusion bypasses endosomes completely, preventing immediate degradation. Therefore, liposomes with highly fusogenic characteristics, were successfully developed at the research center of Jülich, called fusogenic liposomes (FLs).

Nanoparticles surface are covered with proteins immediately after being injected in the blood stream creating the so called “protein corona” (PC). The new biological identity of the nanoparticles - pharmacokinetics and the pharmacodynamics properties- is highly depending on the PC composition. Some certain protein corona components, can cover the liposome from the target receptors, or it can activate the immune system such as immunoglobulin G (IgG) or complement, which stimulate the rapid clearance of nanoparticles from the bloodstream by reticuloendothelial cells [8]. The short blood circulation time is one of the main obstacles to develop new therapeutic treatments based on nanoparticles.

Here the aim of this study is to identify the interactions, structural and functional properties of the Immunoglobulin IgG as a carrier for fusogenic liposomes. Dynamic and electrophoretic light scattering (DLS and ELS, respectively), fluorescence spectroscopy, and Isothermal titration calorimetry (ITC) have been chosen as investigation techniques.

1.2 Hypothesis

The working hypothesis is that fusogenic liposomes (FL) injected into the bloodstream build temporary complexes with blood serum proteins, preventing undesirable fusions. It is important to investigate, characterize and obtained the physicochemical properties of the blood protein/liposomes complexes for their future medical applications.

In this research, we aim to investigate the interaction between different liposomal formulations and the immune protein family immunoglobulin (IgG). Here, we used three different liposomal formulations, the first one is the Fusogenic liposome (FL) which is composed of a lipid mixture of cationic, neutral lipids, and an aromatic molecule at a molar ratio of 1/1/0.1 mol/mol. Cationic lipid: 1,2-dioleoyl-3-trimethylammonium-propane (DOTAP). Due to the positive charge of DOTAP, liposomes are more likely to adsorb to the cellular surface. Neutral unsaturated lipid: 1,2-dioleoyl-sn-glycero-3-phosphoethanolamine (DOPE). The DOPE has a conical structure that serves here as a helper lipid for membrane fusion [9] (**Table 3.2**). Aromatic ring: 1′-dioctadecyl-3,3,3′,3′-tetramethylindotricarbocyanine iodide ("DiR"; DiIC18). The addition of aromatic molecules with cationic liposomes highly increase fusion efficiency [9]. FL liposomes have a cationic charge, so we expected them to adsorb many proteins (IgG). As a control, we designed a second formulation of neutral unsaturated lipids 1,2-dioleoyl-sn-glycero-3-phosphocholine (DOPC) with a hydrocarbon chain length (i.e. 18 C) similar to cationic DOTAP.

Generally, PEGylation can prolong circulation lifetimes by evading the immune system. However, some studies have shown that PEGylation can improve protein binding, and trigger an immune response, thus facilitating liposome clearance. In order to draw a general conclusion, we synthesized a PEGylated DOPC lipids composed of neutral unsaturated (DOPC), and 1,2-dioleoyl-3-phosphoethanolamine-N-[methoxy(polyethyleneglycol)-2000] (ammonium salt) (DOPE-PEG (2000)) at a molar ratio of 1/0.05 mol/mol.

Upon interaction with Immunoglobulin IgG. IgG will cover some liposome formulations surface, which depends on a wide parameter including liposome charge, size, and exposure time [6]. The following techniques has been used to investigate the interaction: Dynamic and Electrophoretic light scattering (DLS and ELS respectively), Isothermal titration calorimetry (ITC), and Fluorescence Spectroscopy.

1.3 Significance of the Work

Due to the permanently increasing applications of nanoparticles as drug carriers in pharmacology and molecular medicine, it is important to understand the driving forces behind the interactions between blood serum proteins and nanoparticles in detail for improving the drug delivery efficiency. Following intravenous administration of nanoparticles, those particles come into close contact with serum proteins of the blood stream. The composition of nanoparticles determines the formation of protein corona, a layer on the surface of nanoparticles composed of several serum proteins. This corona creates a new bio-identity of nanoparticles influencing their circulation in the blood stream, their uptake in different tissues, and their cleavage through the reticuloendothelial system. Therefore, it is necessary to consider the effects of the physicochemical properties of those nanoparticles on the formation of protein corona.

The immune recognition of the liposomes plays a key role in the clearance of the nanoparticles by the reticuloendothelial system. Distinct proteins, such as immunoglobulin G (IgG) or complement factors attached to the liposomal surface can accelerate their opsonization and clearance [10]. Moreover, unspecific immune response can also be released by abundant IgG attached to the nanoparticle surface. Hence NPs application as a drug carrier will end without the achievement of a pharmaceutical effect. However, the presence of IgG on nanoparticles has been reported frequently[3], [11], their interaction is poorly understood on the molecular scale. Therefore, our study aims to fill the gap and elucidate this important interaction in more detail.

1.4 Aims of the Study

In this research, we aim to investigate the interaction between liposomes with different compositions and surface characteristics and the immune protein family immunoglobulin on the molecular level. During our study, liposomes with neutral and positive charges as well as neutral liposomes with covalently bound polymer layers on their surface will be incubated with the human serum protein family immunoglobulin G (IgG). To gain insight into the interactions between those liposomes and IgG, the following analysis have been carried out:

1. Identification the presence of IgG on the liposomal surfaces using dynamic and electrophoretic light scattering.
2. Determination of the thermal stability and IgG affinity to liposomes using isothermal titration calorimetry (ITC).
3. Characterization of the conformational change of IgG in the present of liposomes using fluorescence spectroscopy.

Chapter 2: Literature Review and Theoretical Background

2.1 Biology Approach

2.1.1 Human Plasma Proteins with Special Focus on Immunoglobulin

Human blood plasma contains nearly 3700 identified proteins [12] among other physiologically relevant compounds e.g. hormones, electrolytes, glycose or clotting factors. The numerous proteins are involved in several physiological processes, such as coagulation, immune response, molecular transport, osmotic balance or tissue leakage [13], [14]. For instance, fibrinogen is one of the most important proteins involved in coagulation processes while serum albumin is responsible for maintaining the osmotic pressure in the blood. Apolipoproteins are involved in the transport of lipids and fatty acids, globulins transport hormones and participate in immune reactions [14], [15].

Antibodies or Immunoglobulins (Igs) are involved in the immune response to viral, cellular pathogens and autoimmune diseases, and stimulate an immune response against bound antigens. Immunoglobulins represent one of the main part of the globulins and are produced by plasma cells deriving from B cells [16], [17]. Depending on their biological functions and structures, they can be classified into the following five groups: IgA, IgM, IgE, IgD, and IgG. IgM and IgG with a mean plasma concentration of 1.5 mg/ml and 13.5 mg/ml in normal person respectively [14] can activate complement factors and increase blood clearance of the NPs by macrophages [18]. IgG is one of the most abundant immunoglobulins in blood with 10-20% fraction of plasma proteins [19]. Immunoglobulins are glycoproteins containing 82 to 96% protein and 4 to 18% carbohydrates [20]. A single immunoglobulin (antibody) consists of approximately 100 amino acids [21].

The basic IgG molecule have a "Y-shaped", and consists of four-chain structures, comprising two identical heavy (H) chains and two light (L) chains, as shown in (**Figure 2.1**). The two parts are linked by inter-chain disulfide bonds within the hinge region. Five classes of immunoglobulin exist in humans, each with a different heavy-chain structure (**Table 2.1**). There are four subclasses of immunoglobulins in blood. They are IgG1, IgG2, IgG3, and IgG4, in decreasing order of abundance [20]. The fragment antigen-binding region (Fab) contains the paratope, which is involved in the antigen binding originated from a pathogen. During antigen-antibody formation (Ag-Ab) a conformational change of IgG molecule known as "clicking open" occurs, as has been observed using electron microscopy [22], [23]. The other part of the molecule formed by the lower hinge region and the CH2/CH3 domains is called fragment crystalline (Fc). The Fc part is responsible for effector functions of antibodies, as it contains a largely overlapping binding site for macrophages, neutrophils, and B cell lymphocytes [22]. Moreover, all IgG contain a glycosylation site contributing to the structural conformation of the Fc region [19], [24].

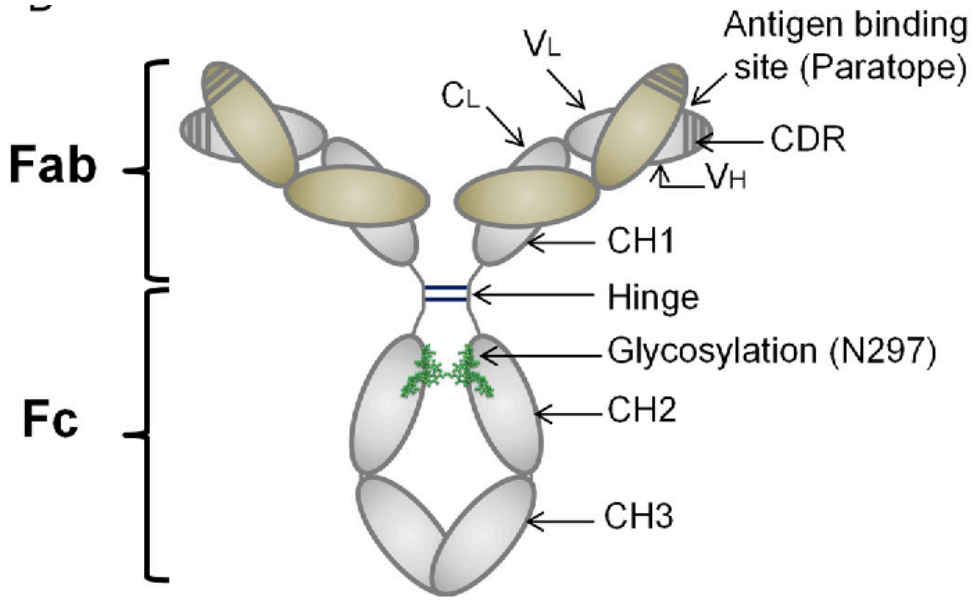

Figure 2.1: Basic structure of an immunoglobulin G molecule [24]. A single immunoglobulin is made up of two identical hydrophilic F_{ab} segments connected by a hinge region to one hydrophobic Fc segment, resulting in a Y-shaped conformation [21].

Table 2.1: General differences in human IgG subclasses [10].

General property	IgG1	IgG2	IgG3	IgG4
Molecular mass (KD)	146	146	170	146
Amine acid in the hinge region	15	12	62	12
Mean level (g/l) in adult	2	4	11	02
Relative abundance	6.98	3.8	0.51	0.56
Half-life in days	21	21	21	21

2.1.2 Liposomal Drug Delivery Structure and Properties

Liposomes were discovered in the 1960s by Bangham [25]. They are formed by spherically closed single (unilamellar) or multiple (multilamellar) lipid bilayers enclosing an internal aqueous space as shown in (**Figure 2.2**) [26]. The bilayer consists of amphipathic phospholipids containing hydrophobic, long fatty acid chains and hydrophilic head groups. The acyl chains are oriented towards each other to minimize interaction with the aqueous solvent, while the hydrophilic head groups are in direct contact with the aqueous environment[26]–[29]. Depending on their size, they are classified as small (d <100 nm), large (100 nm < d <1 μm), and giant (d >1 μm) unilamellar vesicles (SUV, LUV, and GUV, respectively).

Especially SUVs became very popular in medical and pharmacological research, after the approval of the first liposomal drug formulation under the name Doxil. It contained the anti-cancer drug doxorubicin and was used to treat AIDS -related Kaposi's sarcoma [12]. Liposomes have several advantages as drug carriers, e.g. high biocompatibility, reduced toxicity, suitability for hydrophilic as well as hydrophobic drug delivery [30], [31]. Moreover, they are able to accumulate in tumor tissues locally increasing the drug concentration inside the tumor compared

to normal tissues and increase the pharmaceutical effect [26], [32]. Therefore, they have been frequently used as carriers for other anti-cancer drugs such as cisplatin or taxols [33], [34].

In the last decades, cationic liposomes attracted special attention based on their role in gene delivery and vaccination (e.g. COVID-19 vaccine) [27]. Here, the cationic liposomes made of neutral phospholipids and cationic lipids, such as 1,2-dioleoyl-3-trimethylammonium-propane (DOTAP), form complexes, so-called lipoplexes, with the negatively charged nucleic acids via electrostatic interactions. The positively charged complexes can adhere and accumulate on the negatively charged cellular surface and are internalized by endocytosis. In the next step, the complexes have to be released from the endosomes into the cell cytoplasm to reach the nucleus afterwards, where the information can be processed. The endosomal release of the lipoplexes can be facilitated by the lipid composition. Phosphoethanolamines are frequently used as helper lipids. Such lipids have small head groups and large chain regions resulting in a conical molecular shape [28]. The typical inverted conical structure of phosphoethanolamines destabilizes the endosomal membranes which mainly contains phosphocholines with cylindrical geometry forming lamellar membranes [9] and facilitates endosomal escape of the lipoplexes into the cell cytoplasm [27].

Liposomes used for drug delivery purposes are predominantly administrated by intravenous injection. Upon injection, the delivery vehicles come into close contact with blood cells as well as with the blood serum containing hundreds of biomolecules that may adsorb on the liposomal surface. Some of them, e.g. immunoglobulins, enhance the blood clearance by increasing the liposomal uptake by macrophages in the liver and spleen where they will be metabolized [12], [30], [35].

To overcome the uptake process of liposomes by the reticuloendothelial system (RES), a new liposome class was developed. Here, the liposomal surface is coated with an inert polymer shell inhibiting serum protein adsorption on the particle surface as shown in (**Figure 2.2c**).

Consequently, liposomal recognition by macrophages as well as their renal clearance are reduced. Simultaneously, their circulation time in the bloodstream is prolonged [22]. Polymers such as polyethyleneimine, polyxyethylene and polyaspartamide derivatives are frequently used for this purpose [36]. However, the most popular coating polymer is polyethylene glycol (PEG) with a general structure of $H-(O-CH_2-CH_2)_n-OH$. This amphipathic polymer is composed of repeating units of ethylene glycol resulting in different molecular weights (i.e. 2, 8, 20 KDa) and shapes (linear or branched). The more PEG chains, the more hydroxyl groups formed between the polymer and the biofluid, increasing the water solubility of the polymer, decreasing particle aggregation, and minimizing protein adsorption on the PEG surface [22], [37], [38]. If the polymer is covalently coupled to phospholipid molecules, liposomal surface functionalisation can be realized in a more reliable manner compared to simple polymer surface adsorption. In this case, the chemical characteristics of both molecules, the lipid and the polymer, have to be considered by estimating their pharmacological effect. Maruyama and co-workers analysed the circulation time of several lipid-coupled PEGs with different molecular weights (1, 2, 5, 12 KDa) and found that the DSPE coupled PEG with a molecular weight of 2 KDa had the longest circulation time and the highest concentrations in the bloodstream of mice (40% of the dose) after 6 h of injection [39].

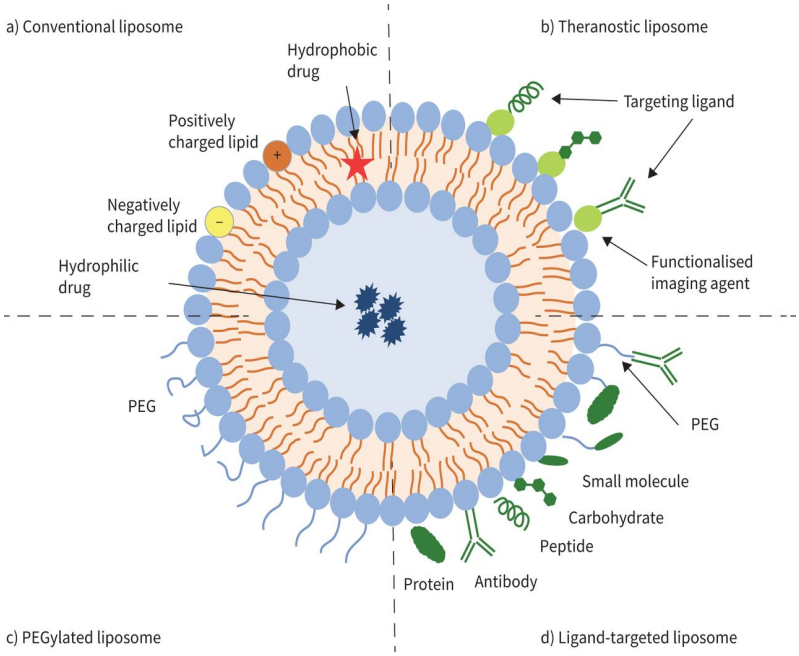

Figure 2.2: Structure of liposomes for drug delivery [40].

2.1.3 Fusogenic Liposomes

Liposomal drug delivery vehicles are taken up by endocytosis, the most common uptake route of mammalian cells. The main drawback of the endocytic uptake pathway is the high degradation rate of the cargo in the lysosomes [41] (**Figure 2.3**). To circumvent cellular endocytosis and simultaneously decrease drug degradation before reaching the target organelles is a major biotechnological challenge. One of the alternative approaches is based on an effective membrane fusion between the carrier and the cellular plasma membrane within a few minutes. Due to the extraordinary high fusion efficiency, such carriers are called fusogenic liposomes (FL) [4], shown in (**Figure 2.3**). They consist of a lipid mixture of cationic1,2-dioleoyl-3-trimethylammonium-propane (DOTAP), neutral lipids 1,2-dioleoyl-sn-glycero-3-phosphoethanolamine (DOPE), and an aromatic molecule 1,1′-dioctadecyl-3,3,3′,3′-tetramethylindotricarbocyanine iodide (“DiR”; DiIC18). At a molar ratio of 1/1/0.1 mol/mol[9]. The positive surface charge of such liposomes facilitates their adsorption on the cellular surface allowing fusion intermediates formation by the two membrane partners. Interestingly, cationic

liposomes without aromatic molecules barely show membrane fusion. The addition of an aromatic compound to the cationic lipid mixture makes the bilayer highly fusogenic [4], [9]. The unsaturated neutral lipid DOPE with a conical molecular shape has a fusion efficiency of 87% (s.d. 8%) (i.e. DMPE, DPPE,…etc.) as investigated by Kolašinac et al. 2018. Kolašinac and co-workers characterize the role of neutral lipids in cell fusion by measuring the fusion efficiency of different neutral lipids i.e. DMPE, DPPE, DOPE, DMPC,…etc in FLs with CHO cells [9].The reason for this interesting physicochemical effect has to be elucidated in more detail in future analysis.

However, the protein-free membrane fusion mechanism is not fully understood, fusogenic liposomes can be applied for molecular delivery purposes. Proteins [1], anti-cancer therapeutics [42], functionalized lipids, DNA vectors as well as mRNA and siRNA [2] biopolymers have been successfully loaded into fusogenic liposomes and delivered into mammalian cells in vitro [1], [2], subsequently as well as in vivo applications [43].

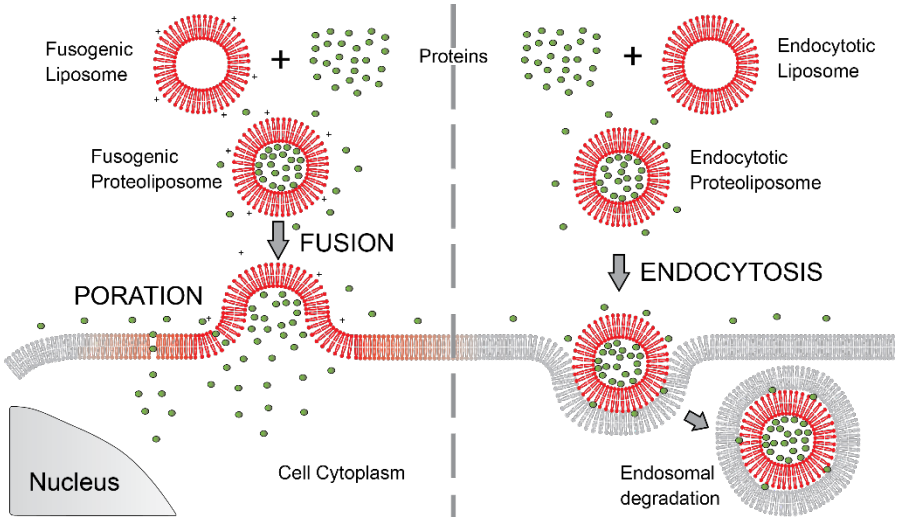

Figure 2.3: Comparison of molecular delivery via fusion and endocytosis [41].

2.2 Interactions of Liposomes with Plasma Proteins

Liposomal drug delivery vehicles are predominantly administrated in the blood stream. Therefore, the interactions between nanoparticles (NPs) in general, and liposomes in special, with plasma proteins have been widely investigated in the last decades. When NPs enter the bloodstream, a rich layer of proteins, called protein corona (PC) forms on their surface. The adsorbed proteins determine the biological identity of the liposomes. Particle distribution, circulation time, stability, cellular uptake, and cleavage are only some of the phenomena strongly influenced by the protein molecules [15], [18], [44].

The protein corona composition depends on the binding affinity of the proteins to the NPs [12]. When proteins with high affinity adsorb on the NP surface, they are tightly bound and have a long lifetime. These proteins form the hard corona. Proteins with low binding affinity and short lifetime form the so-called soft corona [14], [15]. Protein-protein interactions frequently lead to displacement of the first adsorbed abundant proteins by proteins with higher binding affinity. The displacement occurs within milliseconds [45], but the corona composition may continue to change over a longer time [46]. The phenomenon has been observed by Vroman and known as the "Vroman effect" [15].

The composition of the protein corona plays a crucial role in the biological action of liposomes either by promoting liposomal uptake by macrophages (opsonisation) and impairing coagulation, or by inhibiting phagocytosis (dyopsonisation) [12], [14], [36]. Protein adsorption on the particle surface is determined by environmental conditions, such as temperature of biological fluids, the duration of incubation, and the ionic conditions [12], [46], as well as the chemical composition, surface area, size and charge of the NPs [14], [15]. Pioneer et al. analysed the correlation between the liposomal size and charge and the amount of adsorbed proteins, the so-called protein binding value (P_B (g protein/mol lipid)) [7]. He found the lowest P_B value of 30 g/mol for neutral liposomes such as DMPC, since most plasma proteins are negatively

charged at physiological pH. Consequently, the highest P_B value over of 500 g/mol were reported for cationic liposomes containing 1,2-dioleoyl-3-N, N,N-trimethylaminepropane chloride (DOTMA) as positively charged lipid [14]. **Prozeller et al. 2020** found that there is a correlation between the surface charge distributions of proteins and their interaction with NPs. Prozeller and co-workers investigated the Igs interaction with different charge polystyrene nanoparticles [3]. **Figure 2.4** indicate the charge distribution mab of IgG. Hence, we assumed that the nonhomogeneous distribution of charges in IgG would interct differently with NPs.

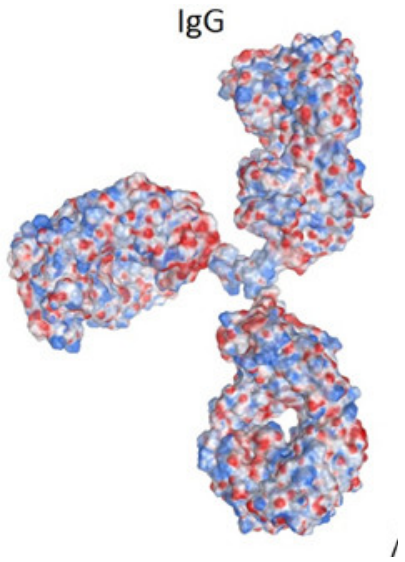

Figure 2.4: Surface charge distribution maps of IgG. In the graphic, negatively charged patches (red areas), positively charged patches (blue areas), and neutral charges (white areas) [3].

2.2.1 Interactions of PEGylated Liposomes with Plasma Proteins

Polyethylene glycol (PEG) is a hydrophilic polymer with a chemical structure of $(CH_2CH_2O)_n$, and a molecular weight of 2000-5000(KDa.) [7]. Phosphatidylethanolamine is usually coupled to the PEG. The chains of PEG form a hydration layer through hydrogen bonds, with neighboring water molecules. PEGylated surfaces can prevent the adsorption of nonspecific

proteins i.e. opsonins proteins. Thus, increasing the stability, and avoiding the rapid clearance of the NPs [47]. Consequently, PEG is one of the most relevant artificial polymer used for surface coating of liposomes. The United States Food and Drug Administration (US FDA) has approved about 20 PEG polymers without safety concerns [48]. By grafting PEG on the liposomal surface, protein adsorption can be significantly reduced, resulting in less macrophage cellular uptake and prolonged blood circulation time [12]. Semple and co-corkers (**Figure 2.5**) demonstrated that plasma proteins are less likely to adhere on liposome surfaces coated with PEG using aqueous two-phase partitioning techniques. By adding 5% DSPE-PEG to liposomes (2000 KDa), P_B values were reduced significantly (Semple et al. 1998).

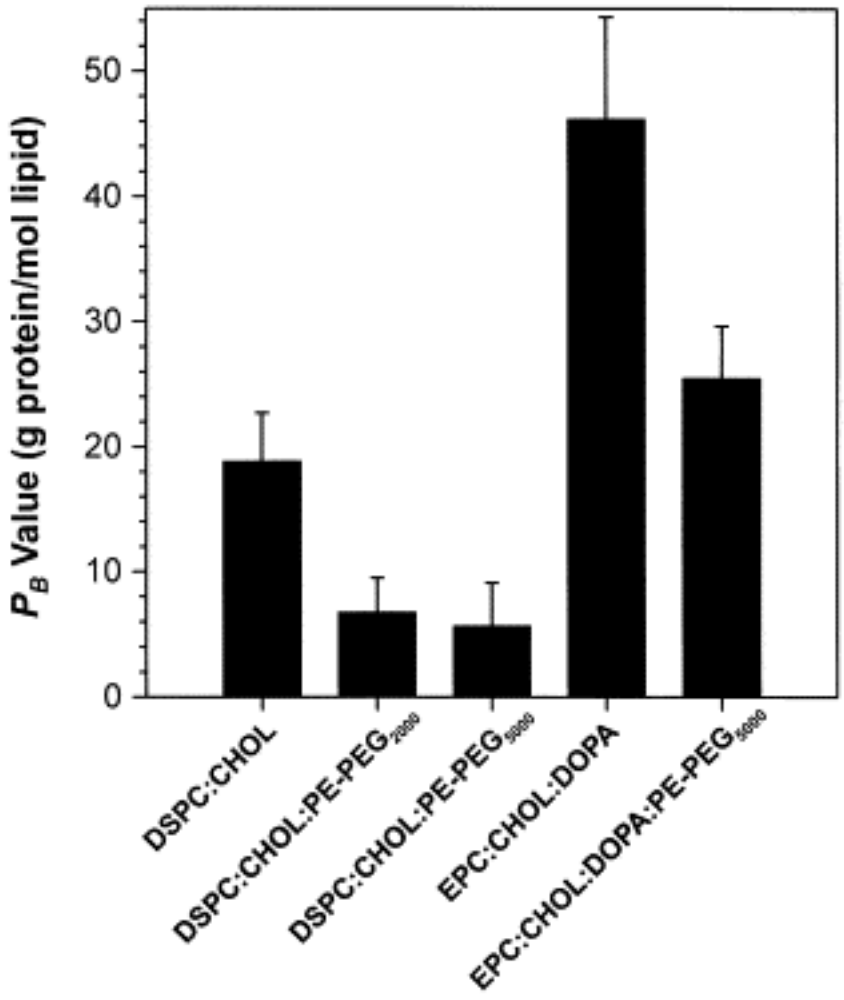

Figure 2.5: P_B values of liposomal formulation with and without the DOPE-PEG [7].

However, many studies have reported about PEG polymer applications with very low toxicity, pegylation can also reduce transfection potency by increasing the cellular uptake of nanoparticles [49], which is known as "PEG dilemma.". Unexpected immune responses upon repeated treatments have been observed frequently [50]. Especially IgM and IgG showed high binding affinity to PEGylated nanoparticles releasing high particles clearance by RES [12]. A relative protein abundance (RPA) of ca. 15% of immunoglobulins was even found on PEGylated liposomal surfaces [6]. Huckabyet and co-corkers characterized the binding of IgG1 with PEG using x-ray crystallography and determined conformational changes of the Fab-tag of the protein. Simultaneously, the PEG polymer also showed conformational changes by wrapping itself around the IgG1-ring backbone increasing surface contact area with the Fab-tag and stabilizing the complex [48]. Here, flexible PEG polymer chains without any covalent bond to the particle surface have been analysed. Recent studies about PEGs covalently bound to e.g. lipid molecules are missing.

2.2.2 Interactions of Cationic Liposomes with Plasma Proteins

Cationic liposomes interact with negatively charged plasma proteins such as fibrinogen and vitronectin (opsonins) predominantly, while on liposomal surfaces made of phosphoethanolamines proteins such as serum albumin or apolipoproteins (dyopsonins) adhere [12]. Giulimondi and co-workers compared the protein corona of cationic, neutral and anionic liposomes after incubation in human plasma using mass spectroscopy [5]. Their results showed that the relative protein abundance (RPA) of plasma proteins identified on neutral liposomes surface did not show significant differences at physiological protein concentration (50% serum) while the protein bond to cationic liposomes increases significantly with increasing protein concentration. Most of the adhered proteins had a molecular weight of 30 to 100 KDa and an isoelectric point below 7. Moreover, coagulation proteins, such as fibrinogenes, and lipoproteins were found to be the most abundant proteins on all liposomal surfaces. The RPA of immunoglobulines was determined at 2-4%. In comparison, Caracciolo´s analysis revealed ca. 20% of immunoglobulins adhered on cationic liposome surfaces as the most abundant protein

[6]. Simultaneously, (**Figure 2.6**) Gronemann et al. found apolipoproteins (Apo) with ca. 40% of RPA value as the most determinant protein compound adhered on fusogenic liposomes and only 10% of immunoglobulins (Ig) [51]. However, numerous studies have reported about the presence of immune proteins on cationic liposomal surfaces upon incubation with blood plasma, none of them gave deep insight into the binding characteristics of those two partners, a lipid molecule with positive charge and the immunoglobulin.

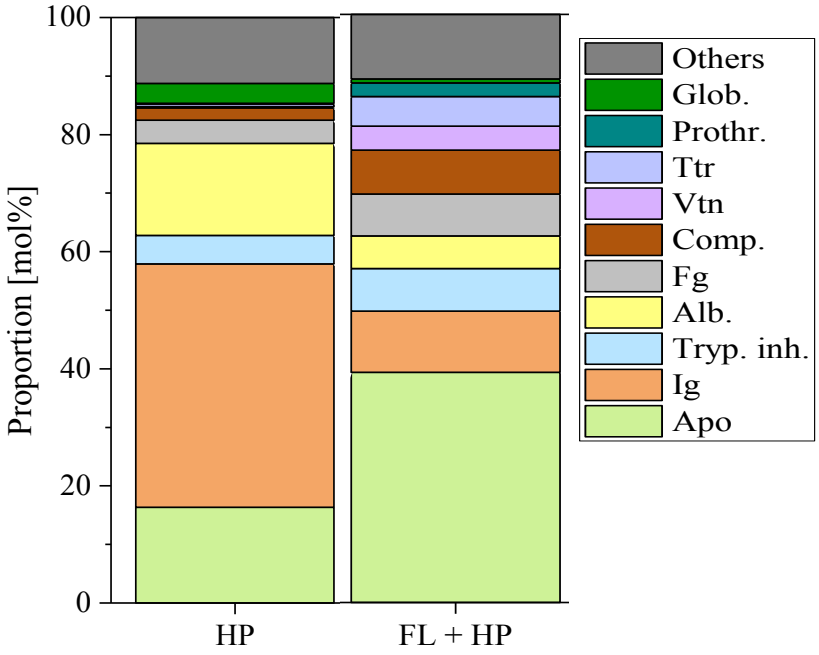

Figure 2.6: Using mass spectroscopy. (Left) molar proportion of proteins found in the human plasma. (Right) molar proportion of proteins adhered on the surface of FL after incubated with human plasma for 30 min at RT [51].

2.4 Related Studies

(Gronemann, 2021): Using mass spectroscopy Gronemann incubated FL with human plasma at RT for 30min. He found that apolipoproteins (Apo) was the most determinant protein

compound adhered on fusogenic liposomes with ca. 40% as value of relative protein abundance and only 10% of immunoglobulins (Ig) found on the FL surface (Gronemann 2021).

(Huckaby et al. 2020): Huckabyet and co-corkers characterized the binding of IgG1 with PEG polymer chains using x-ray crystallography. They determined the conformational changes of the Fab-tag in the protein. In addition, the PEG polymer also exhibited conformational changes by wrapping itself around IgG1 ring backbones increasing the surface contact area with the Fab-tag and stabilizing the complex. A flexible polymer chain without any covalent bond to the particle surface was analyzed here [48].

(Kayser et al., 2011): A spectroscopic study of the human IgG was conducted using fluorescence to examine the Trp solvent accessibility of different Trp classes using Acrylamide as a quencher. They found that IgG1 contains Tryptophan residues which are randomly distributed over the protein and can be classified according to their water accessibility within the IgG1 (**Table2.2**). Additionally, these residues have different lifetimes depending on their position and contribute differently to the overall protein fluorescence, though that contribution is further influenced by their surrounding polarity.

In their study they have a non-liner Stern-Volmer plot indicating that more than one Trp class is contribute to the overall fluorescence. The partially examine residue quenched by the Acrylamide but less than the surface-examine residues as they have higher availability to the molecule solvent. The fractional quenching was 52% using the modified Stern-Volmer equation. The buried residues didn't quench by the Acrylamide. They also found that the Energy transfer between theses residues could be the only mechanism for their emission, but it might occur where the Trp- Trp distance is $\leq (10 - 15\ A^{\circ})$ (Kayser et al. 2011).

Table 2.2: Class of tryptophan residues (Trps) with their life-time and maximum emission wavelenght

Trp class	$\tau(ns)$	$\lambda(nm)$
Surface	3.6	> 340
Partially buried	1.45	$320 - 340$
Buried	0.27	≤ 320

(Caracciolo et al. 2014): Caracciolo´s and co-workers analyzed two liposomal formulations: [DOTAP and PEG], and the second one: [DOTAP (30%),DSPC(50%), and CHO(20%)] with a final concentration of (1 mg/ml) for each formulation. They incubated them with Human (HP) and Mouse Plasma (MP) at 37℃ for 1h. Their analysis revealed that:

1. The Protein Corona formed is influenced by the physiological environment and the Nanoparticle composition.
2. Size and zeta potential measurements show that both PEGylated and un-PEGylated DOTAP liposomes incubated with HP were about 70 and 60 nm larger in size than bare liposomes respectively. The zeta measurements support the existence of the liposome-protein complex. The authors suggest that the protein binding in PEGylated DOTAP was caused by the high PEG density used (10%).
3. Mass spectroscopy revealed ca. 20%, and 15% of immunoglobulins adhered on cationic, and PEGylated liposomal surfaces respectively [6].

(Prozeller et al. 2020): Prozeller and cowarkers studied the interaction of different human immunoglobulin classes, IgG, IgA and IgM with different charge polystyrene nanoparticles (PS-NPs) including: PS-NPs (-10 mV), PS-NPs-COOH (-29 mV), and PS-NPs-NH_2 (+2 mV), with small amount of polyethylene glycol for each NPs for stabilization. Their study revealed that:

1. Using reducing SDS-PAGE, they found that IgG was adsorbed on all PS-NPs surfaces. This result was further supported by a more negative value in zeta potential value.
2. Upon interaction of IgG with charged NPs-PS, an aggregation processes were observed.
3. There is a correlation between the surface charge distributions of Igs and their interaction with NPs
4. ITC titrations suggest that IgG undergo more hydrophobic interactions with PS-NPs. while hydrophilic interactions i.e. electrostatic interactions take place for the functionalized NPs [3].

(Giulimondi et al. 2020): They incubated Cationic (DOTAP) , Anionic 1,2-dioleoyl- sn-glycero-3-phospho-(1′-rac-glycerol) (DOPG), and Neutral (DOPC) liposomes with Human plasma (HP) in increasing protein concentration from 1% to 50%.

1. The Protein corona (PC) of DOPC is slightly affected by increasing protein concentration, while the protein bond to DOTAP and DOPG increases significantly with increasing protein concentration.
2. As protein concentrations increase (1% - 50%), proteins bond to NPs in nanograms of protein per milligram of lipid were as follow: (3 -15.8) for DOTAP, (0.22 - 1.33) for DOPC and (0.28 - 2.53) for DOPG.
3. The PC of DOTAP was primarily composed of IgG1, HPT, IGK, IGL1, A1AT, and APOA1 [5].

(Weissmann et al. 1974): Weissmann and co-workers studied the interaction between cationic liposomes with native and aggregated IgG using column chromatography. Aggregated IgG was prepared by heating native IgG for 10 min at 61.5℃ to simulate their configuration in immune response. Upon incubated a 0.15 mg IgG /ml of cationic liposomes for 10 min at room temperature, the mixture was subjected to chromatography, they found that:

1. Cationic liposomes bind about 50% of the native protein, while over 75% of aggregated IgG interact with the bilayers.
2. The Fc part of the IgG is responsible for the interaction with liposomes membrane.
3. Aggregated IgG-liposome interactions can be explained by conformational changes in IgG, or by the formation of many Fc portions that can insert into the bilayer, such interactions are hydrophobic in nature.[22]

(Sangrà et al. 2017): They study the interaction between neutral and PEGylated large-unilamelar liposomes (LUVs) and magneto-liposomes (MLs) upon incubation with 1 mg/ml Bovine Serum Albumin (BSA) at 37c for 24 h. Phosphatydylcholine (PC) or (DMPC) is the main component of phospholipids with 20% of cholesterol. Their study revealed that:

1. Size measurements show small changes in all samples, and the aggregation process was observed in samples containing PC. Zeta potential shifted toward a more negative value than the bare liposomes. A thin layer of BSA is present on the liposome surface.

2. Fluorescence quenching results revealed that the quenching effect was observed in all samples, with a negative deviation in the Stern-Volumer plot consequence to aggregation in LUVs or MLs at high concentrations of lipids.

3. In the ITC analysis, no significant binding was found and no thermodynamic parameters were determined. Experiments yielded titration patterns with endothermic energy contributions.

4. Hydrophobic interactions dominate in BSA-PC systems, while electrostatic interactions dominate in BSA-PEGylated systems [49].

(Anbazhagan et al. 2011): They studied the interaction of the main protein in Bovine plasma (PDC-109) with different lipids membrane. The lipids consisting of phosphatidylcholine such as dimyristoyl phosphatidylcholine (DMPC), dipalmitoyl phosphatidylcholine (DPPC), dimyristoyl phosphatidyl-glycerol (DMPG). Using isothermal titration calorimetry (ITC) 0.25 mM of PDC-109 was injection into 0.08 mM phosphatidylcholine suspensions at a different temperature, they found that:

1. The interaction between PDC-109 and the lipids membrane is hydrophobic, entropically driven (endothermic binding).
2. With increasing temperature, the number of binding sites (n) decreases, while enthalpy and entropy increase.
3. The binding of PDC-109 to lipids in the gel phase was endothermic. But in the liquid crystalline phase, DMPC exhibited a complex binding with PDC-109 (endothermic and exothermic).

Chapter 3: Material and Data Acquisitions

The following subchapters provide an overview of all substances used throughout this thesis. The first section covers chemicals, materials, and instruments. The second section describes the methods of preparing liposomes and provide an overview of the techniques used for acquiring data, along with a description of sample preparation conditions for each of the characterization techniques (DLS, ELS, Fluorescence Spectroscopy, and ITC).

The substances were used without further purification. Ultrapure water was produced using the Arium® Pro Ultrapure Water System from Sartorius (Göttingen, Germany).

3.1 Materials

3.1.1 Lipids

Lipids were purchased from Avanti Polar Lipids, Inc. (Alabaster, AL, USA) in chloroform at 10 mg/mL with purity > 99%: 1,2-dioleoyl-sn-glycero-3-phosphoethanolamine (DOPE), 1,2-dioleoyl-3-trimethylammonium-propane; chloride salt (DOTAP), 1,2-dioleoyl-sn-glycero-3-phosphocholine (DOPC), and 1,2-dioleoyl-sn-glycero-3-phosphoethanolamine-N-[methoxy(polyethyleneglycol)-2000] (ammonium salt) (DOPE-PEG(2000)), DOPE-PEG was diluted in chloroform to 1 mg/ml. The carbocyanine dye 1,1′-dioctadecyl-3,3,3′,3′-tetramethylindotricarbocyanine iodide ("DiR"; $DiIC_{18}(7)$) was ordered from Thermo-Fisher Scientific (Waltham, MA, USA), and was diluted in chloroform to 1 mg/ml. Lipids stock solutions were stored at-20℃. All lipids are listed in (**Table 3.1)**. Chemicals structures of the lipids are shown in (**Table 3.2)**.

Table 3.1: Lipid components for liposome preparation with their IUPAC and molecular weight

Lipid	IUPAC name	Mw [g/mol]
DOPC	1,2-dioleoyl-sn-glycero-3-phosphocholine	786.113
DOPE	1,2-dioleoyl-sn-glycero-3-phosphoethanolamine	744.034
DOPE-PEG	1,2-dioleoyl-sn-glycero-3-phosphoethanolamine-N [methoxy(polyethyleneglycol)-2000 (ammonium salt)	3234.11
DOTAP	1,2-dioleoyl-3-trimethylammonium-propane; chloride salt	698.542
DiR	1,1′-dioctadecyl-3,3,3′,3′-tetramethylindotricarbocyanine iodide	1013.41

Table 3.2: Lipid components for liposome preparation with their structure and fluorescence spectra (orange) of DiR

Lipid	Structure	Molecular Shape
DOPC	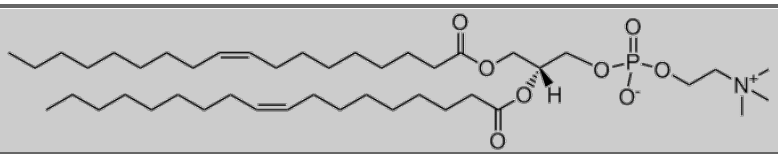	Cylindrical
DOPE	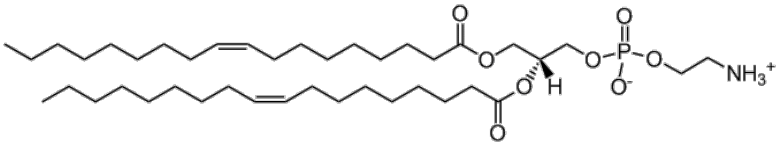	Conical
DOPE-PEG	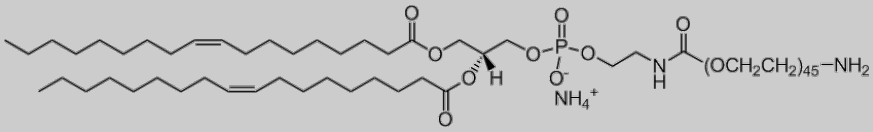	Conical
DOTAP	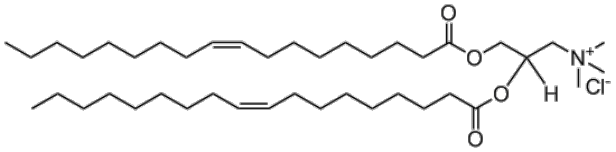	Cylindrical
DiR	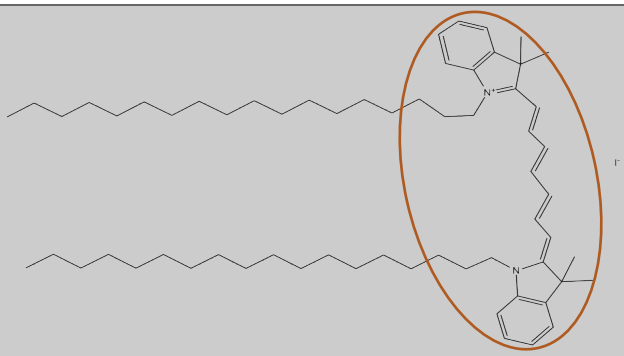	Cylindrical

3.1.2 Protein

Incubation experiments were based on lyophilized human IgG from Sigma-Aldrich, (Taufkirchen, Germany), with a molecular weight of 150 kDa. The IgG was stored at 4°C.

3.1.3 Buffers (Phosphate-Buffered Saline (PBS), HEPES)

Buffers were prepared in purified water, all components were obtained from Sigma-Aldrich, (Taufkirchen, Germany), pH was adjusted with aqueous solutions of HCl (1mM) or NaOH (1mM). Buffer osmolalities were determined using a freezing point osmometer (Osmomat 030, Gonotec GmbH, Berlin, Germany) (HEPES-30 m osm/kg, PBS-292 m osm/kg). Buffers were filtered using an Acrodisc®syringe filter manufactured by Pall Corporation (Port Washington, New York, USA), and stored at 4 °C until use.

Phosphate-Buffered Saline (1× PBS), pH 7.4; 1× PBS was prepared by dissolving the reagents listed in (**Table 3.3**) in 800 mL of purified water. To reach a pH of 7.4, a solution of HCL (1mM) or NaOH (1mM) was added along with water to make a 1L solution. PBS was Stored at 4 °C.

Table 3.3: The Reagents used for (**1x**) of PBS solution.

Components	Concentrations (mM)	Mw (g/mol)	Amount added(mg)
NaCL	137	58.44	8006.0
KCL	2.7	74.55	95.7
Na_2HPO_4	8.1	141.19	1143.6
KH_2PO_4	1.47	136.08	200.1

2-(4-(2-hydroxyethyl)-1-piperazinyl)-ethanesulfonic acid (HEPES-Buffer), pH 7.4; as standard liposomal buffer, HEPES was used. To make 100 mL of 20 mM HEPES, pH 7.4. 476.6 mg of HEPES (238.3 g/mol) was dissolved in 80 mL of water overnight. The pH was then adjusted to 7.4 using a solution of HCL (1mM) or NaOH (1mM) was added along with water to make a 0.1 L solution. HEPES was Stored at 4 °C.

3.1.4 Instruments

Below are listed the research instruments used in the study.

Table 3.4: List of instruments used in the research

Hardware	Company
Dynamic light scattering and Zeta potential measurement system (Zetasizer Nano ZS)	Malvern Instruments, Malvern, UK
Spectrofluorometer (Spectrometer Fluorolog-3)	Horiba Jobin Yvon, Kyoto, Japan
Isothermal titration calorimetry (ITC)	Malvern Instruments, Malvern, UK

3.2 Methods

The following subsections provide an overview of the experimental procedures underlying the applied analytical techniques.

3.2.1 Preparation of Liposomes

In this study, three different kinds of liposomes were used. In all cases, liposomes were prepared according to the method described by [53]. Briefly lipids were mixed in chloroform (Merck Millipore, Darmstadt, Germany) at the desired ratio (**Table 3.5**). The chloroform was evaporated under vacuum for at least 30 min. Dry lipid film was hydrated with HEPES buffer to a total lipid concentration of 2 mg/ml and homogenized by vortexing for approximately 1-2 min to produce multilamellar liposomes. FL Liposomes were further sonicated in an ultrasonic bath (Sonocool, Bandelin electronic GmbH, Berlin, Germany) for 20 min at 4 to 6°C. On the other side DOPC and DOPC-PEG liposomes suspensions were extruded 20 times through a 100 nm polycarbonate filter using Avanti Mini Extruder (Alabaster, AL, USA), to form unilamellar vesicles with a mean diameter of 100-150 nm. Extrusion was carried out at 23°C, which is above the phase transition temperature of DOPC (-20°C), and DOPC-PEG.

Prepared liposomes were kept at 4°C. If storage times exceeded one day, the ultrasonic treatment was repeated immediately before use.

Table 3.5: Lipids composition of formed liposomes.

System	Abbreviation	Lipid composition	Molar lipid ratio
Cationic liposomes (Fusogenic liposomes)	FL	DOTAP/DOPE/DiR	1/1/0.1
Neutral liposomes	DOPC	DOPC	1
Stealth liposomes	DOPC-PEG	DOPC/DOPE-PEG	1/0.05

3.2.2 Dynamic Light Scattering (DLS)-Theory

Dynamic light scattering, also known as photon correlation spectroscopy (PCS) or quasi-elastic light scattering (QELS), is a material characterization technique for determining particles size distribution of colloidal samples. During the measurement, the sample is illuminated by a monochromatic laser and the scattered light intensity is recorded with a photon detector at a fixed or variable scattering angle [54]–[56]. On this time scale, intensity fluctuations reflect the rate of fluctuation of the particles. The fluctuation in the scattering intensity is used to calculate the size distribution of particles within the sample. Fluctuations are captured using the method of autocorrelation, in which the scattered intensity at time t is compared to itself at time $t + \tau$, where τ is the correlation delay time. The process is repeated over the period of observation and for a (typically logarithmically spaced) range of values τ to generate a correlation function. From the decay of the correlation function, the rate of diffusion (D) is calculated [54], [55]:

$$\Gamma = q^2 D \quad (1)$$

Where Γ is the exponential decay rate, and q is the scattering vector defined by the scattering angle and wavelength of the light. After decay rates has been extracted, the size distribution can be achieved by Stokes–Einstein equation that's relate D to the hydrodynamic diameter (d_H) of the particle [54], [55]:

$$d_H = \frac{KT}{3\pi\eta D} \quad (2)$$

In this equation, k denotes the Boltzmann constant, T the absolute temperature, and η the viscosity of the medium. The quantity d_H is the diameter of an equivalent rigid sphere that diffuses at the same rate as the analyte.

3.2.3 Dynamic Light Scattering (DLS)-Measurements

DLS was used to detect Immunoglobulin G (IgG) bound to liposome surface complexes marked by an increase in liposome size. Here the hydrodynamic diameter of liposomes and IgG/liposome complexes was measured using the Zetasizer Nanodevice ZS (Malvern Instruments, Malvern, UK). Instrument control and data analysis were performed using Malvern's Zetasizer software.

Preparation of Liposomes for DLS Measurements; for characterization of bare liposomes, liposome stock solutions (2 mg/ml) were diluted 1/10 with filtered PBS, to a final concentration of 0.2 mg/ml, and measurements were performed at room temperature (**Figure 3.1**).

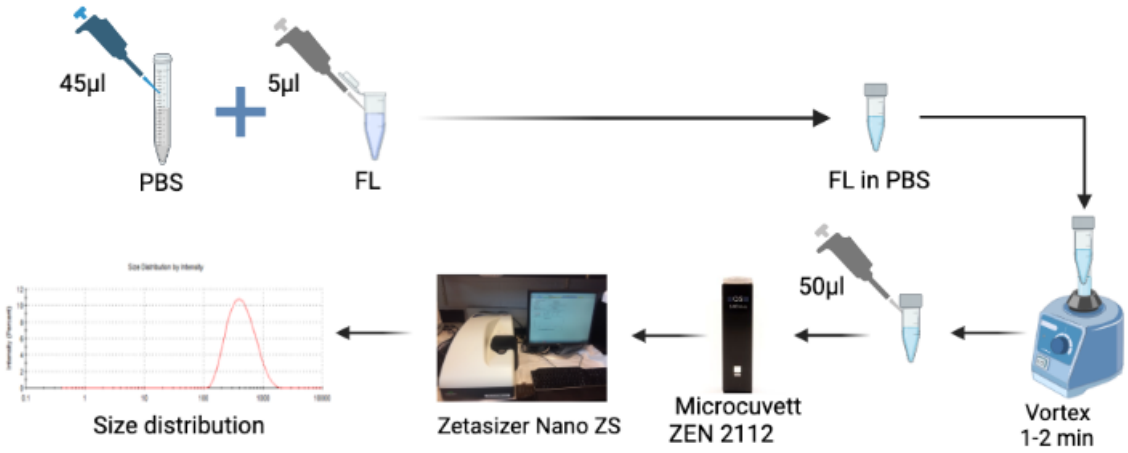

Figure 3.1: DLS measurements. Bare liposomes FL (2 mg/ml) were mixed with PBS. After that FL (0.2 mg/ml) vortexed for 1-2 min to mix well and then filled in microcuvette (50 µL) to analyzed on the DLS at 23°C.This process was repeated for DOPC and DOPC-PEG.

Preparation of Liposome/IgG Complex for DLS Measurements; to analyze the IgG/liposome complexes, liposomes were incubated with IgG at a molar ratio of 1/0.01 mol/mol. Here 1 µl of the liposome stock solutions (2 mg/ml), were mixed with 16 µl of IgG (2.5 mg/mL) and incubated at 37°C for 30 minutes in a vacuum heating and drying oven from ThermoFisher Scientific (Waltham, Massachusetts, USA). After incubation, the dispersion of IgG/liposome complexes was diluted to 50 µl with PBS and measured immediately afterward (**Figure 3.2**).

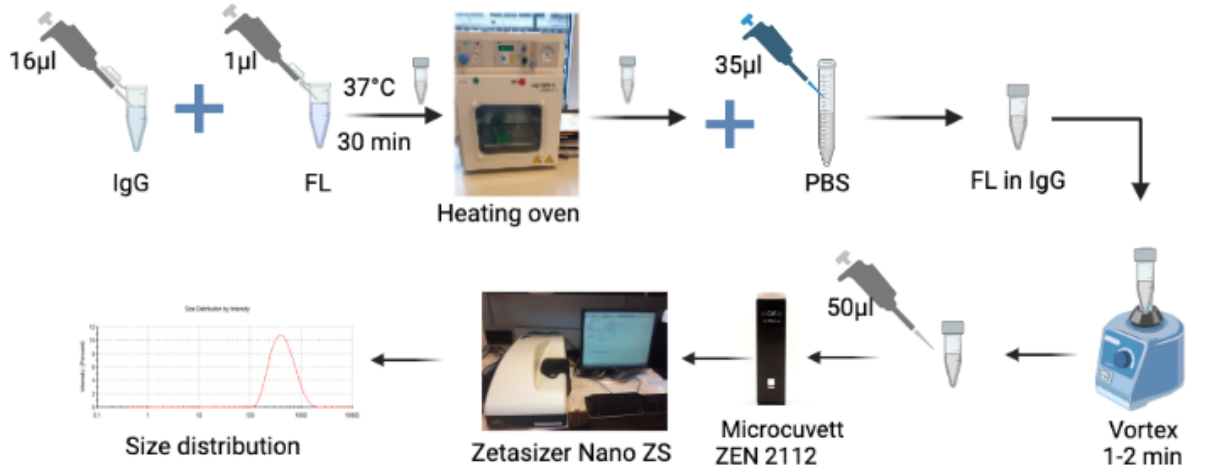

Figure 3.2: DLS measurements for IgG/FL complex, 1 µL of FL (2 mg/ml) was added to 16 µL of IgG (2.5 mg/ml) and incubated at 37°C for 30 minutes in a heating oven. The dispersion was diluted to 50 µl with PBS and measured immediately afterward. This process was repeated for DOPC and DOPC-PEG.

Experiment Setup; the prepared samples were filled bubble-free in a cleaned and solvent-rinsed quartz microcuvette with a path length of 3 mm purchased from Hellma (Muellheim, Germany) (**Figure 3.1 and 3.2)**. The cuvette was cleaned between measurements by thorough rinsing with ethanol and water. All measurements were performed in backscatter mode at 173 °angle.

The measurements provided the polydispersity index (PDI) of the sample and the underlying size distribution. The data reported are the mean peak position within the size distribution and the standard deviation of at least three independently prepared samples.

3.2.4 Electrophoretic Light Scattering (ELS)-Theory

Electrophoretic light scattering is a technique to determine the zeta potential (ζ) distribution of particles in a colloidal sample. The zeta potential, also termed as electro-kinetic potential, is the potential at the slipping plane of a colloid particle moving in an electric field [56]. When a charged particle is dispersed in a medium, an electric double layer develops on its surface. The

inner layer consists predominantly of ions with opposite charge to that of the particle surface (Stern layer). These ions are strongly bound to the surface. In the outer layer the binding ions are less firmly attached [54], [56].

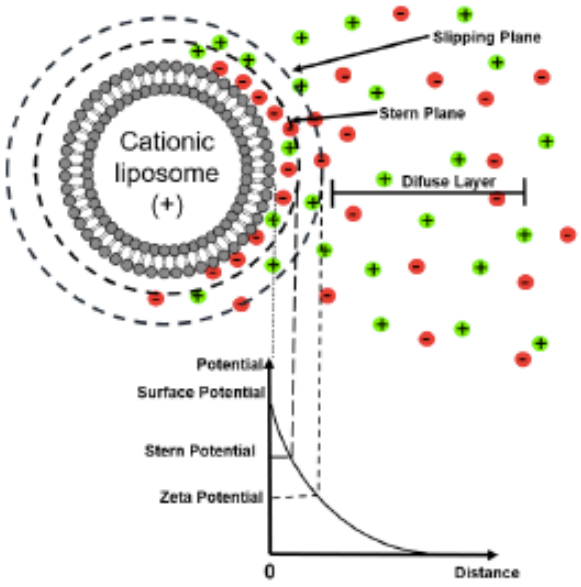

Figure 3.3: Schematic representation of zeta potential [57].

When an electric field is applied across an electrolyte, charged particles move towards the oppositely charged electrode (electrophoresis). Ions within the boundary move with the particles, while ions beyond the boundary do not. This boundary is called as the surface of hydrodynamic shear or slipping plane and schematically illustrated in (**Figure 3.3**).

Simultaneously, viscous forces acting on the particles tend to oppose this movement. When equilibrium is reached between these two forces, the particles move with constant velocity (electrophoretic mobility-U_E). The potential that exists at the slipping boundary is known as the zeta potential and can be calculated via Henry equation [54], [56]:

$$U_E = \frac{2\varepsilon\,\zeta\,f(\kappa a)}{3\eta} \tag{3}$$

Where ζ denotes the zeta potential, U_E the electrophoretic mobility of the particles, ε the dielectric constant, η the viscosity of the buffer, and $f(\kappa a)$ the Henry's function. Here, two approximations are generally used: in an aqueous solution with moderate electrolyte concentration, the f (κa) =1.5 referred to as the Smoluchowski approximation. For small particles in low dielectric constant media, (κa) =1.0 and referred to as the Huckel approximation. Upon measuring the electrophoretic mobility of the dispersed particles their zeta potential can be calculated.

3.2.5 Electrophoretic Light Scattering (ELS) -Measurements

The surface charge of liposomes and protein/liposome complexes was measured using the Nano-Zetasizer (Malvern Instruments Inc, Malvern, UK). Instrument control and data analysis were performed using Malvern's Zetasizer software.

Samples Preparation; for zeta potential measurements, DLS samples were diluted to 800 µl with PBS. Detailed information on sample preparation can be found in subsection 3.2.3. **(Figure 3.1)** 800 µL of the diluted dispersion was pipetted bubble-free into a Malvern disposable capillary cell (DTS1070).

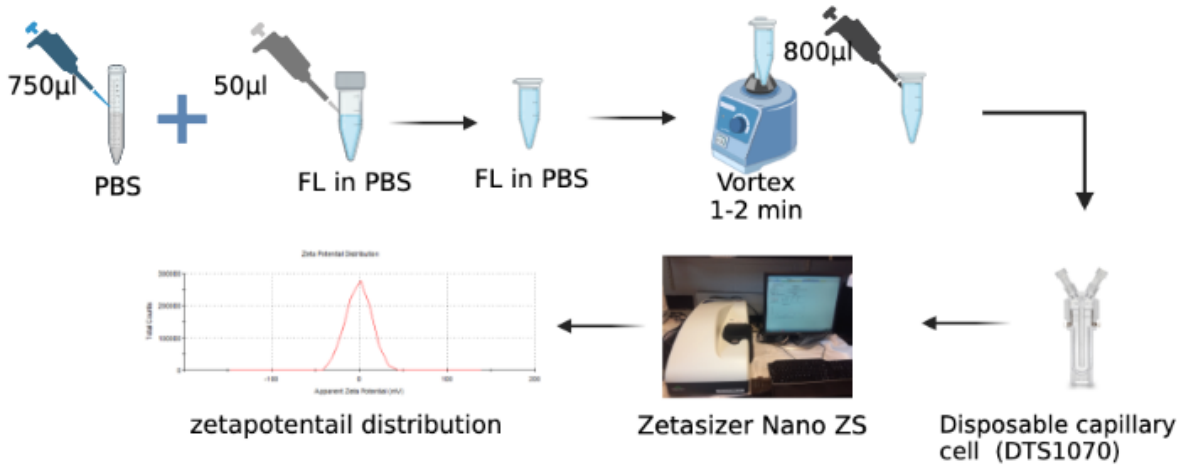

Figure 3.4: Zeta measurements before incubating with IgG. DLS samples were diluted to 800 µl with PBS using the same device just after the DLS measurements represents IgG/liposomes complex. Same measurements were repeated for DOPC and DOPC-PEG. All NPs were measured again after the incubation in the same way.

Experiment Setup; the cell was thoroughly cleaned with ethanol and water and pre-rinsed with the solvent of interest before use. All measurements were performed at 25 °C. The number of scans was manually set to 12 and the Smoluchowski approximation was selected as the model for data analysis.

Based on the collected data, the software provided the average zeta potential value and the underlying potential distribution. The data reported are the mean zeta potential value and standard deviation taken over at least three independently prepared samples.

3.2.6 Fluorescence Spectroscopy-Theory

Fluorescence spectroscopy analyses fluorescence from a molecule (fluorophores) based on its fluorescent properties. Typically, aromatic molecules i.e. Tryptophan (Trp), phenylalanine (Phe), and tyrosine (Tyr). Fluorescence is a type of luminescence caused by photons exciting a

molecule, raising it to an electronic excited state. In excited singlet states, the electron in the excited orbital has the opposite spin orientation as the ground-state electron. Hence, the opposite spin allowed the return to the ground state (S_0) resulting in the emission of a photon. The emission rates of fluorescence are on the order of nanoseconds [58]. Jablonski's diagram describes the processes through the absorption and emission of light (**Figure 3.5**). The electronic level (singlet ground, first, and second) are labelled as S_0, S_1, and S_2, respectively. These electronic energy transitions involve vibrational energy levels depicted by 0, 1, 2 …etc, in which Fluorophores can be found throughout. The transitions between states are depicted as vertical lines and occur in femtosecond timescale [58].

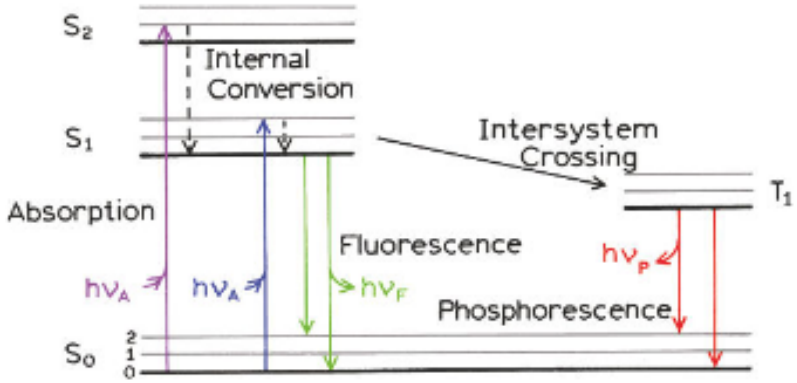

Figure 3.5: Jablonski diagram [58].

A molecule can absorb a photon which contains energy equal to the difference between its ground state and one of its excited states, the energy of a photon is given by:

$$E = hv \tag{4}$$

Where h is Planck's constant, and v is the frequency of the light.

Fluorophore is typically excited as a result of light absorption from S_0 to a higher vibrational state (S_1 or S_2), followed by rapid relaxation to the lowest vibrational level of S_1, a process called an internal conversion, which occur in picoseconds timescale or less. Return to S_0 usually results in an excited vibrational state at the level of the S_0, which then relaxes within picoseconds [58]. The emitted light is usually at longer wavelengths (lower energy) than the absorbed light; this difference is called the Stokes-shift (**Figure 3.6**) [59].

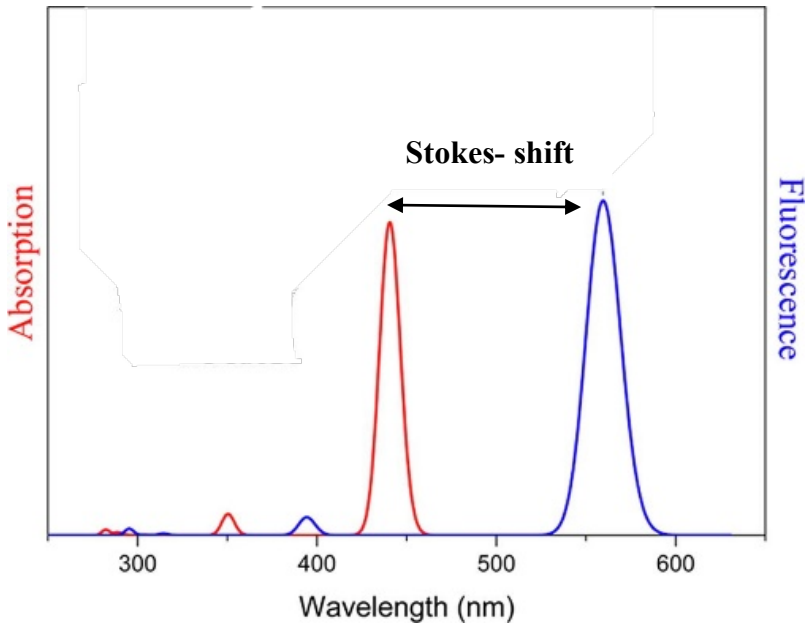

Figure 3.6: Characteristic of stokes- shift, edited from [60].

A plot of emission against wavelength for any given excitation wavelength is known as the emission spectrum. If the wavelength of the exciting light is changed and the emission from the sample plotted against the wavelength of exciting light, the result is known as the excitation spectrum. Furthermore, if the intensity of exciting light is kept constant as its wavelength is changed, the plot of emission against exciting wavelength is known as the corrected excitation spectrum. The quantum efficiency of most complex molecules is independent of the wavelength of exciting light and the emission will be directly related to the molecular extinction coefficient of the compound; in other words, the corrected excitation spectrum of a substance will be the same as its absorption spectrum [61].

Static and Dynamic Quenching; Fluorescence intensity can be reduced by a process called quenching, which occurs through different mechanisms i.e. ground-state complex formation, energy transfer, collisional quenching etc. Collisional or dynamic quenching takes place when a fluorophore in the excited-state come in close contact with some other molecule in the solution, consequently the fluorophore is no longer fluorescence-active (**Figure 3.7**). Here the molecule caused the deactivation called the quencher. Hence, fluorophore returned to the ground state without emitting a photon. In the process, molecules are chemically unchanged. Regard to the collisional quenching, the reduction in the fluorescence intensity is defined by the well-known Stern-Volmer equation:

$$\frac{I_0}{I} = 1 + K_{SV}[Q] = 1 + k_q\tau_0[Q] \qquad (5)$$

Where I_0 and I are the fluorescent intestines in the absence and presence of quencher respectively, K_{SV}: The Stern-Volmer quenching constant which indicate the accessibility of the fluorophore to the quencher, where larger values of the quenching constant K_{SV} indicate that the fluorophore moves freely in the solution or is located on the biomolecule surface. k_q is a bimolecular quenching constant, τ_0 :the unquenched lifetime, and $[Q]$ is the quencher concentration.

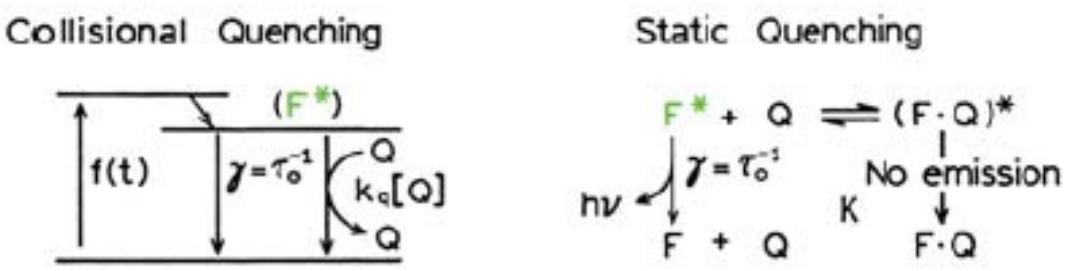

Figure 3.7: Collisional and Static quenching, In the case of static and dynamic quenching the fluorophore and quencher must be in contact to interact. Collisional quenching occurs when the quencher comes into contact with the fluorophore in its excited state, after which the fluorophore returns to its ground state, without emitting a photon. Static quenching occurs when a fluorophore and the quencher form a non-fluorescent complex in the ground state, that's when absorb light the complex return to the ground state without emitting a photon [62]. *Both static and dynamic quenching require a contact between the fluorophore (Trp) and the quencher (FL).

Furthermore, in the ground state, a fluorophore-quencher pair can form a non-fluorescent complex. This process is called static quenching since it does not depend on molecular collisions. [62] Upon absorption of light, this complex returns to the ground state without emitting a photon (**Figure 3.7).** It is possible to distinguish between these two mechanisms based on their different temperature dependence. For dynamic quenching, higher temperatures result in larger diffusion coefficients, which increases the quenching constants. Conversely, higher temperatures reduce the stability of complexes, resulting in a lower static quenching constant [63].

Antibodies usually have many Trp residues, which are randomly distributed. Trp residues contribute to the total protein fluorescence differently. Some residues are located on the protein surface, making them highly accessible to the solvent; while others are located within the protein, with little or no interaction with solvent molecules. Due to their different surroundings, they have a different fluorescence emission: In one type, the fluorescence intensity is maximum at 350 nm, in another at 320 nm, while in the last one, the maximum intensity is around 330–340 nm [52].

IgG contain 26 tryptophan residues and 52 tyrosine residues. Tryptophan's intrinsic fluorescence was used to investigate how the microenvironment of the residues changes as a consequence of liposome/IgG binding [64]. Different liposomal formulations were used as a quencher to examine Trp access to NPs.

Since the quenching constants of the Trp residues present in IgG (**Figure 3.8**) can differ for each emitter group, stern volumer-plot may be nonlinear. Consequently, to better analyze the data we can use a modified Stern-Volmer plot[52]. Using this equation, the differences in accessibilities of tryptophan residues in proteins can be determined using the following equation:

$$\frac{I_0}{I_0 - I} = \frac{1}{f K_a [Q]} + \frac{1}{f} \tag{6}$$

Where I_0, I are flouresecence intensity of protein (IgG) with and without the quencher at a specific wavelength (341nm), K_a:modified Stern-Volmer binding constant, f: fraction of the accessible tryptophan residues fluorophores to the quencher, and [Q] is the quencher concentration.

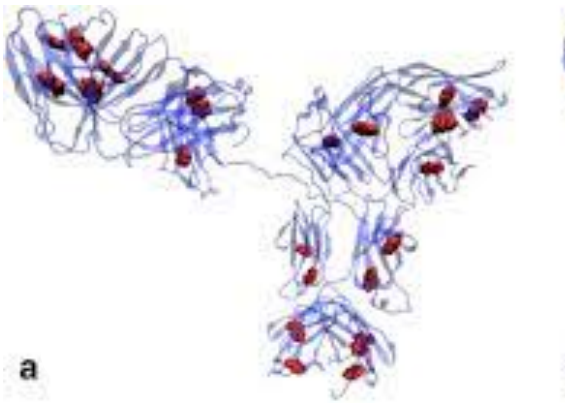

Figure 3.8: The distributed of Trp residues (red) in the IgG1(blue) antibody protein [52].

The fluorescence data were further analyzed to determine the binding constant for FL-IgG interaction using the following equation:

$$\log\frac{I_0 - I}{I} = \log k + n\log[Q] \quad (7)$$

Where I_0, I: fluorescence intensity of IgG with and without the quencher at a specific wavelength (341nm), k: binding constant, n: number of binding sites per IgG molecule, and [Q]: the quencher concentration.

3.2.7 Fluorescence Spectroscopy-Measurements

Fluorescence spectroscopic studies were conducted on Fluorolog-3, HORIBA spectrometer from Jobin Yvon (Bensheim, Germany; Kyoto, Japan). Data analysis and instrument control were performed with Origin Lab software (Northampton, Massachusetts, USA). A spectrum of free IgG and liposome-bound IgG were recorded at 37 °C.

Preparation of Liposome/IgG Complex; (64 µL, 2.5 mg/mL) IgG stock solution was diluted to 2000 µL PBS to yield an IgG concentration of 0.01 mg/ml. A sample of 2000 µL was transferred into a clean SUPRASIL® quartz glass precision cuvette with a path length of 10 mm purchased from Hellma (Müllheim, Germany). A dried FL lipid film was re-dispersed in 20 mM HEPES to obtain a lipid concentration of 2 mg/ml. The fluorescence spectrometer was connected to a thermostat from (Julabo USA, Inc), to maintain a constant temperature of 37 °C. (**Figure 3.9**) shows how the measurements were performed in details for the FL/IgG complex. The same steps were performed for DOPC and DOPC-PEG. Cuvette cleaning involved, thorough cuvette sonicated 10 minutes at room temperature, with water, chloroform, water.

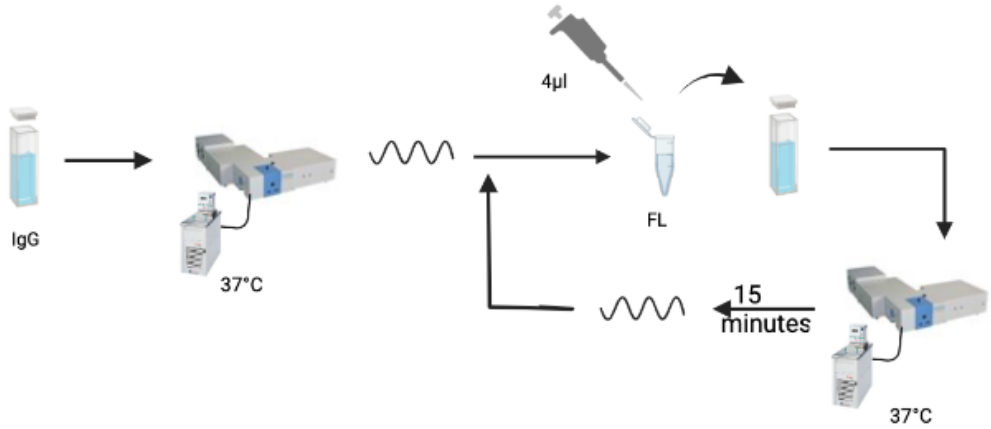

Figure 3.9: IgG (0.01 mg/ml) in 2000 µL of a quartz glass precision cuvette was analyzed on the fluorescence spectrometer at 37°C (using a thermostat connected to the instrument). After that, 4 µL of FL (2 mg/ml) was added to the cuvette yield (0.001 mg/ml), yielding an IgG/lipid molar ratio of 1/0.01 mol/mol . It was then reinserted in the instrument for 15 minutes until it mixed well. The cuvette was equipped with a small magnetic stirrer to ensure homogenous mixing. This process was repeated six times.

Experiment Setup; Tryptophan excitation was performed at a wavelength of 283 nm. Excitation and emission slits were set to a width of 1 and 3, respectively. Emission spectra were recorded between 300 and 550 nm.

Background Correction; The recorded IgG and IgG/liposome spectra were corrected with the spectra of 0.01 mg/mL IgG in PBS as in (**Figure 3.10**) and 0.001 mg/mL liposomes in PBS at 37 °C in the same way like in (**Figure 3.10**), to eliminate scattering effects and possible fluorescence contribution from DiR. Each experiment was repeated at least three times. The difference spectra were averaged over three independent measurements.

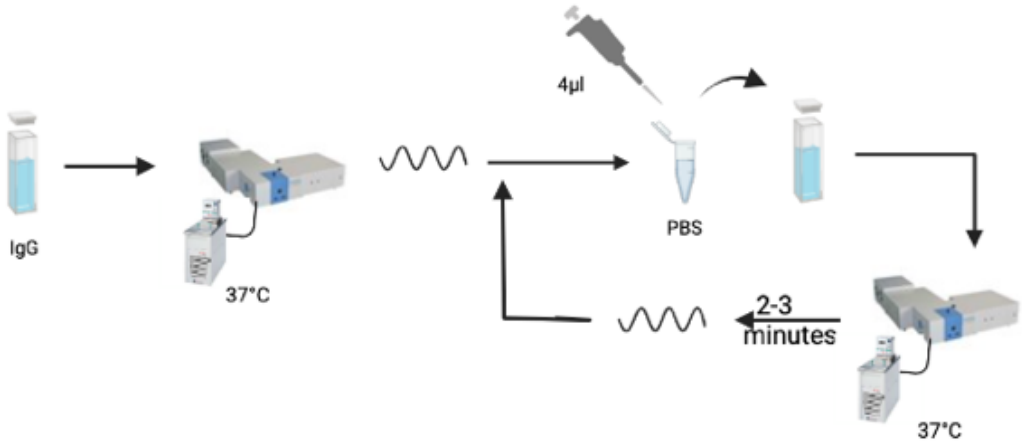

Figure 3.10: IgG (0.01 mg/ml) in 2000 µL of a quartz glass precision cuvette was analyzed on the fluorescence spectrometer at 37°C (using a thermostat connected to the instrument). After that, 4 µL of PBS was added to the cuvette. It was then reinserted in the instrument for 2-3 minutes until it mixed well. The cuvette was equipped with a small magnetic stirrer to ensure homogenous mixing. This process was repeated six times.

3.2.8 Isothermal Titration Calorimetry (ITC) – Theory

Isothermal titration calorimetry (ITC) is one of the physical techniques that directly measures the heat discharged or consumed all along a bimolecular reaction [65]. ITC is a highly sensitive tool for determining, for example, the binding of peptide to lipid membranes [66], [67]. Hence there is no need for biomolecules to be labeled or tagged. Since chemical modifications can potentially interfere with or affect the binding interaction under study. ITC can be applied to almost any size molecule, including small molecular weight antigens, like carbohydrates, as well as large proteins, like immunoglobulin complexes [17].

The instrument consists of two cells **(Figure 3.11 a)**; one is the sample cell containing the macromolecule of interest e.g protein solution and the other is the reference cell for the buffer solution [66], [68]. Both cells are kept at steady temperature and pressure. During the measurement, the ligand is titrated into the sample cell **(Figure 3.11 b)**. Macromolecular binding with the ligand results either in heat discharge or consumption, which causes the change

of temperature within the sample cell. However, the instrument will always maintain the constant temperature in the sample cell equivalent to that of the reference cell **(Figure 3.11 c)**. For maintaining the temperature, the instrument gives relevant power (higher or lower) depending on the interaction [65].

The heat change is then simply calculated by integrating the power over the time (seconds), which gives us the enthalpy of the reaction **(Figure 3.11 d)**. The heat discharged or consumed all along the calorimetric reaction corresponds to the fraction of bound ligand. An increased ligand concentration leads to saturation of substrate and finally less heat is discharged or consumed (**Figure 3.11 c**). The amount of heat discharged upon inclusion of ligand is defined as follows [65]:

$$Q = V_O \Delta H_b [M]_t \left\{ \frac{K_a[L]}{1 + K_a[L]} \right\} \quad (8)$$

Where Q denotes the heat absorbed; V_0 the sample cell volume; ΔH_b the enthalpy of binding per mole of ligand; $[M]_t$ corresponds the total concentration of macromolecule in the sample cell; K_a the binding constant; and [L] is the concentration of the free ligand [65].

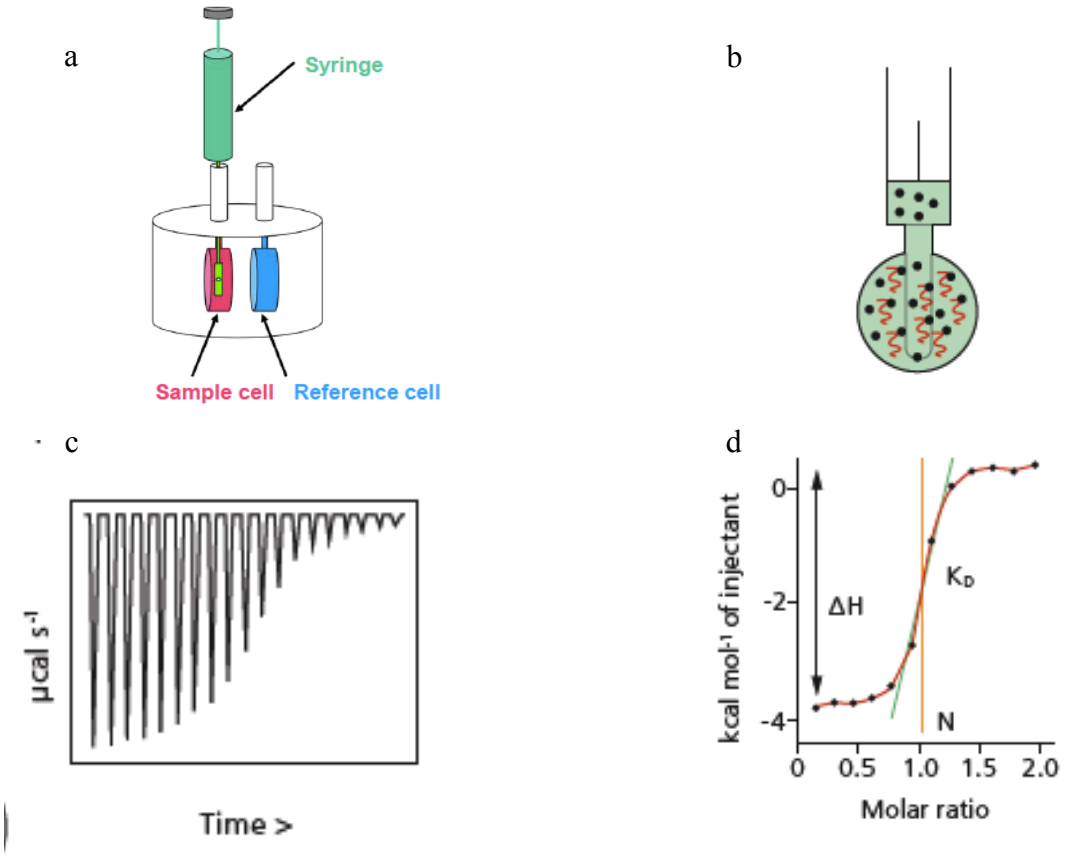

Figure 3.11: The progress of ITC experiment. (a) the ITC consist of syringe (green) contains IgG, sample cell(pink) contains FL and reference cell (blue) contains water. (b) Sample macromolecules (red ribbon) are injected with ligand (black dots), typically in 0.5- 2µL aliquots, until the ligand concentration exceeds the sample concentration. .(c) A heat pulse is generated upon injection of ligand that is integrated over time and normalized for concentration to produce a titration curve of kcal/mol vs molar ratio (ligand/sample). (d) Fitted binding model to determine affinity (KD), stoichiometry (N), and enthalpy of interaction (ΔH) (Srivastava & Yadav, 2019).

ITC can accurately measure the binding affinity (K_D), stoichiometry (N), and enthalpy(ΔH) directly from the experiment. While entropy, and Gibbs free energy can be calculated using the Gibbs free energy equation:

$$\Delta G = \Delta H - T\Delta S = RT \ln K_D \qquad (9)$$

Where $\Delta G, \Delta H$ and ΔS are the changes in free energy, enthalpy, and entropy of binding respectively, T is the absolute temperature in (k), and R is the gas constant.

An enthalpy change (ΔH) occurs when non-covalent bonds are formed or broken i.e. hydrogen and ionic bonds and van der Waals interactions. When there is a new non-covalent bound formed ($-\Delta H$). Entropy (ΔS) is a measure of the system's tendency to become disordered. The interaction between two biomolecules can result in either an orderly state ($-\Delta S$) or a disorderly state ($+\Delta S$). An interaction is triggered when ΔG is negative. The free energy value can be used to compare the affinity of interactions at the same conditions i.e. temperature, buffer, pH, etc. The higher the binding affinity, the lower the K_D value, and the more negative ΔG becomes [17].

3.2.9 Isothermal Titration Calorimetry (ITC) – Measurements

Isothermal titration calorimetric (ITC) measurements were performed at pH 7.40 using MicroCal PEAQITC from Malvern Panalytical (Malvern, Worcestershire, UK). Instrument control and data analysis were accomplished using the associated MicroCal PEAQ-ITC software. The experimental data were fitted to a theoretical titration curve using PEAQ-ITC software, with ΔH (binding enthalpy, kcal mol–1), K_a (association constant), and n (reaction stoichiometry) as adjustable parameters.

Protein (IgG) Dialysis; 4 mL of a PBS (~ 279 mosm/l, pH=7.40) were used for IgG (20 mg/ml) dialysis. In dialysis, only small molecules can diffuse through selectively permeable membranes, separating them from large molecules. IgG was dialyzed against PBS at 4°C for three days to remove any impurities and bound ligands. The dialysis was conducted using a Spectra/Por® dialysis membrane from Repligen (Waltham, Massachusetts, USA) exhibiting a molecular weight cutoff of 25 kDa. During the three days of purification, the entire dialysis medium was replaced. After dialysis, IgG was carefully removed from the membrane and IgG aliquots were stored at -20°C. The PBS left over from dialysis was stored at 4°C.

Pr-Experiment; the reference cell was manually cleaned with methanol and water and then filled with water afterward. The sample cell was washed automatically with an aqueous 10 wt% DECON90 solution and water and was manually rinsed with dialysis buffer thereafter. Afterward, the syringe was washed with DECON90 solutions and water and dried with methanol.

Sample/ Syringe Loading; IgG was titrated in to liposomes in PBS (1x, pH 7.40). A stock solution of 0.15 mM FL was carefully added to the sample cell to avoid bubble formation. In the sample cell, the cleaned syringe was filled with 40 µL of the 1.35 µM IgG stock solution. In addition, the same amount of immunoglobulin solution was titrated into 300 µl of DOPC (12.50 mM) and DOPC-PEG (1250 mM). Each measurement was done once due to the high concentration required and the cost of the IgG.

Experiment Setup; each measurement was performed with 19 injections from a computer-controlled micro-syringe at room temperature. The first protein injection was 0.4 µl followed by 19 * 2 µl injections, separated by 250 s, with a stirring speed of 750 rpm between each injection. The first injection is usually small and neglected from the data analysis, due to the diffusion effect during the temperature equilibration. The reference power was set to 10 µcal/s, and the feedback mode to low. Titrations were performed at pH 7.4 using phosphate-buffered saline.

Background Correction; Since ITC is a highly sensitive instrument, the enthalpy of ITC includes binding heat, as well as buffer/biomolecules ionization heat [17]. Hence for each measurement, the integrated heats of dilution were subtracted. Titrations of IgG in PBS, PBS in PBS, and PBS in liposomes served as references for determining the dilution heat.

Chapter 4: Results and Discussions

4.1 Dynamic and Electrophoretic Light Scattering (DLS) and (ELS)

DLS and ELS analysis were carried out to determine liposomes size and surface charge distributions upon IgG incubation. Especially due to electrostatic attractive forces, an increase of particle size and a change in zeta potential at the same time are to be expected. To figure out the role of electrostatic forces in the IgG–liposomes interactions, bare liposomes at a concentration of 2 mg/ml and liposome-IgG complexes at a molar ratio of 0.01:1 were characterized by dynamic and electrophoretic light scattering. Free IgG at 2.5mg/mL was used as reference **(Figure 4.1)**.

Free IgG; the mean diameter of IgG was found about 12.6 nm (s.d. 0.9 nm) as shown in (**Figure 4.1 a)**. This value was in good agreement with hydrodynamic diameters reported earlier [64], [69]. The second peak at 164 nm indicated protein aggregation processes. As determined by ELS, IgG was neutrally charged, -2 mV (s.d. 0.5 mV) **(Figure 4.1 b)** in PBS buffer underlying aggregation trends in the protein solution.

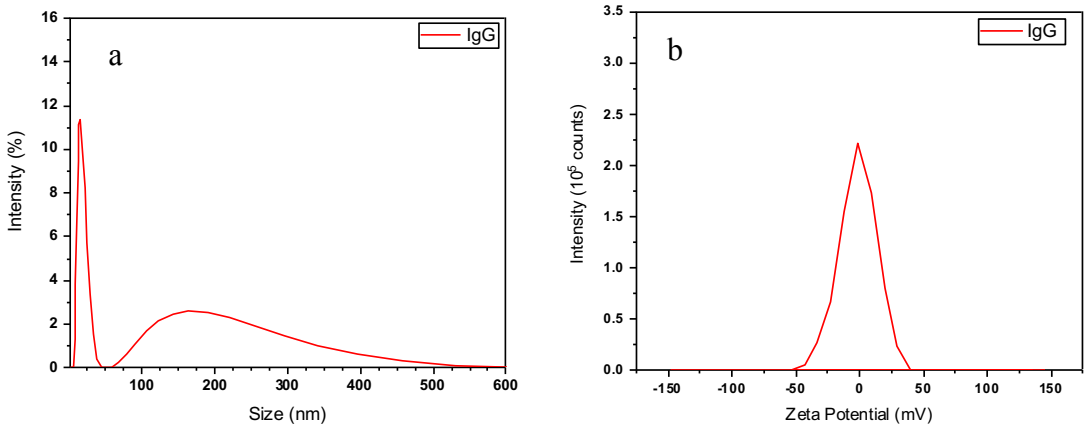

Figure 4.1: (a) Hydrodynamic diameter and (b) zeta potential distribution of IgG in PBS (pH 7.40) at RT

FL/IgG complexes; The hydrodynamic diameter of bare FL was found at 378 nm (s.d. 25 nm). Upon IgG incubation, the diameter distribution peak was shifted to 1056 nm (s.d. 71 nm), indicating a significant increase (Δd = 678 nm) in particle size **(Table 4.1)**. Caracciolo et al. 2014 incubated DOTAP liposomes with HP, where particle size indicating an increase of 60 nm [6]. Considering the small size of IgG protein (13 nm), we assume that this very large size changes cannot be contributed exclusively to IgG accumulates on the liposomal surface, rather to the aggregation of the FL/IgG complexes. This assumption was supported by Oku and co-workers, who incubated cationic liposomes with fetal bovine serum and analyzed the liposomal behavior in the suspension. Their results showed that positively charged liposomes tended to form aggregates in the presence of blood serum [70]. Similar to Oku, Prozeller and co-workers studied also the IgG interaction but with different charged nanoparticles. Their result showed also significant aggregation upon IgG adsorption on charged nanoparticles [3]. Considering those results, it can be assumed that the force involved in the interaction between the FL and the IgG is also of electrostatic nature.

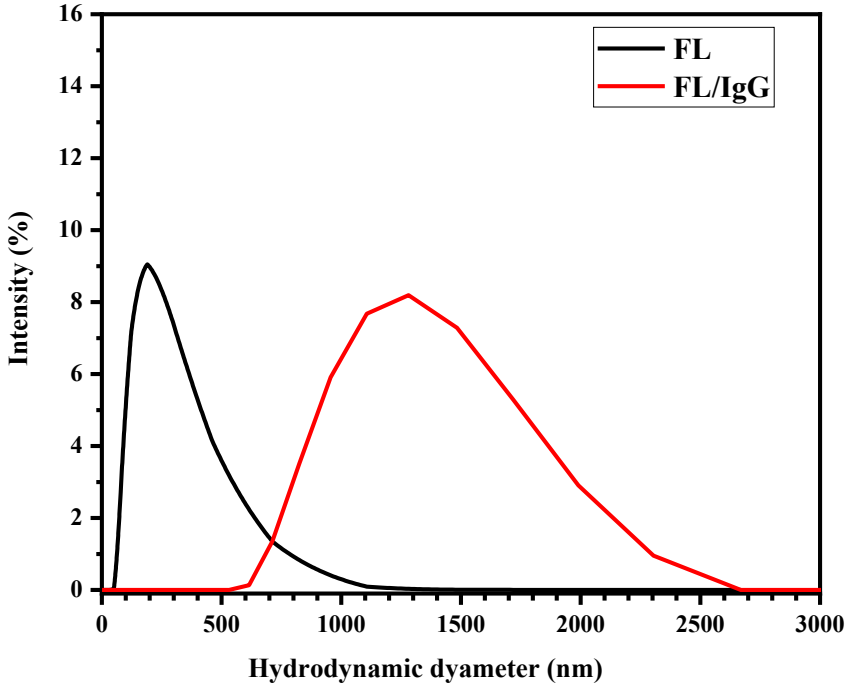

Figure 4.2: Hydrodynamic size distributions of bare FL (black) and FL/IgG complex (red). Measurements were carried out in PBS at 37 °C.

This conclusion is further supported by our zeta potential results (**Figure 4.3**). Here, a decrease in zeta potential was detected **(Table 4.1)**. FL particles showed an overall positive charge (28 mV (s.d. 2.0 mV)) while FL/IgG complexes became neutrally charged (-0.6 mV (s.d. 0.2 mV)) similar to pure IgG. The positive charge of the liposomes was presumably shielded by the negatively charged protein parts while the positively charged protein parts did not interact with the similarly charged liposomes resulting in an overall similar potential distribution like observed in pure IgG solution.

Table 4.1 **:Average hydrodynamic diameter** (d), polydispersity index (PDI) and zeta potential (ξ) of pure FL liposomes and FL/IgG complex in PBS buffer at 20°C. (n=3) The individuals are listed in Appendix (**Table A.1**)

FL **DOTAP/DOPE/DiR**	**IgG**	**d (nm) ± sd**	**PDI± sd**	**ξ (mv) ± sd**
+	-	378 ± 25	0.2 ± 0.0	28.0 ± 2.0
+	+	1056 ± 71	0.9 ± 0.1	-0.6 ± 0.2

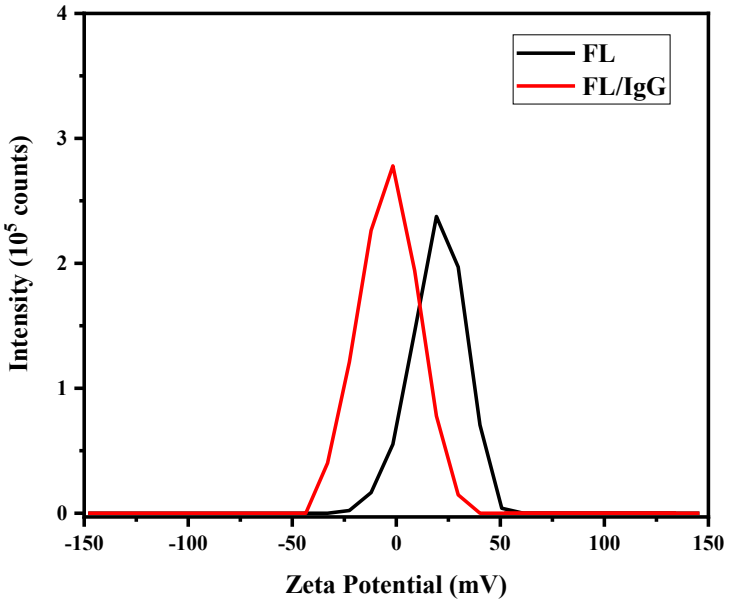

Figure 4.3: Top panel: zeta potential distributions of free IgG. Bottom panel: bare FL liposomes (black) and FL/IgG complex (red). Measurements were carried out in PBS at 37 °C.

DOPC/IgG Complexes; Prior to measurements, DOPC liposomes were extruded using 100 nm pore size filters at room temperature. This step was necessary because neutrally charged DOPC liposomes tend to form multilamellar liposomes with very heterogeneous distribution in size. Upon extrusion, the monomodal distribution of the hydrodynamic diameter with a peak position at 156 nm **(Figure 4.4)** indicated no particle aggregation. The slightly elevated size corresponded to the pore size distribution of the extruder membrane.

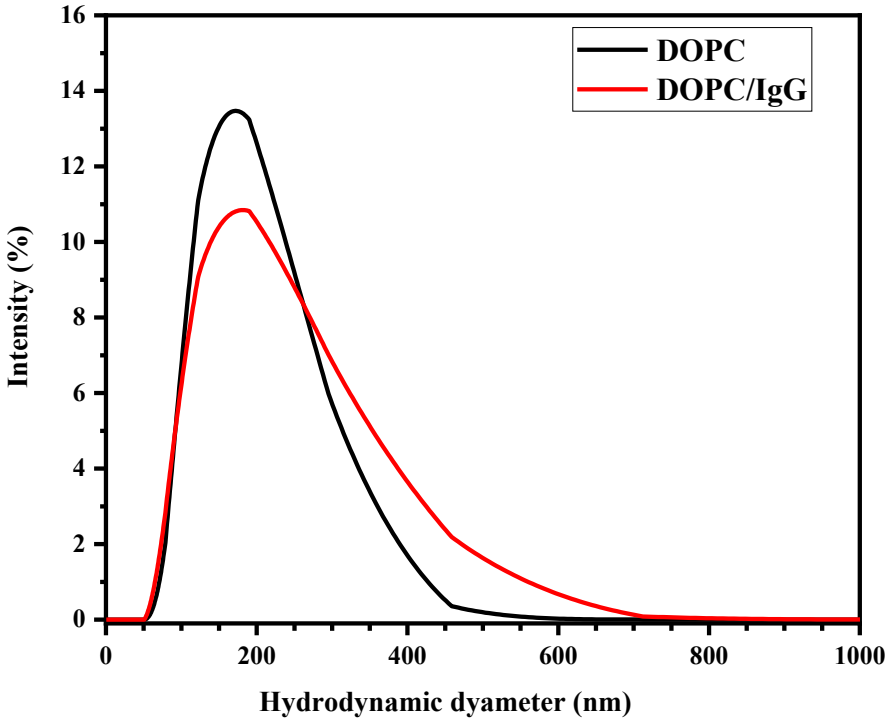

Figure 4.4: Hydrodynamic size and distributions of bare DOPC liposomes (black), and liposome/protein complex DOPC/IgG complex (red). Measurements were in PBS at 37 °C.

Incubation of DOPC liposomes with IgG did not significantly change the hydrodynamic diameter **(Figure 4.4)**. Additionally, no change in the zeta potential was observed as shown in (**Figure 4.5)** and **(Table 4.2)**. These findings indicated no protein adsorption on the surface of DOPC liposomal. Similar result obtained by Giulimondi et al. 2020 who incubated the DOPC liposomes with HP in increasing concentration. They found that DOPC was slightly affected by increasing protein concentration [5].

Table 4.2: **Average hydrodynamic diameter** (d), polydispersity index (PDI) and zeta potential (ξ) of pure DOPC liposomes and DOPC/IgG complex in PBS buffer at 20°C. (n=3) The individuals are listed in Appendix (**Table A.2**).

DOPC	IgG	d (nm) ± sd	PDI± sd	ξ (mv) ± sd
+	-	156 ± 10	0.2 ±0.0	-4 ± 2
+	+	156 ± 10	0.3 ±0.1	-1 ± 0

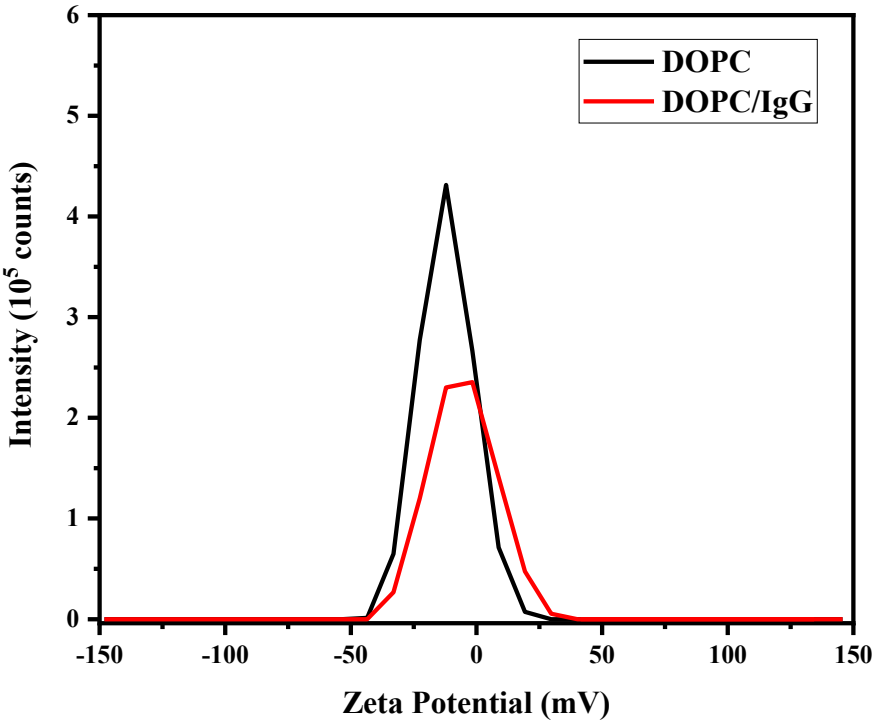

Figure 4.5: Top pane: zeta potential distributions of free IgG. Bottom panel: bare DOPC liposomes (black), and DOPC/IgG complexes (red). Measurements were carried out in PBS at 37 °C.

DOPC-PEG /IgG Complexes; DOPC-PEG liposomes were extruded on the same manner like described by DOPC liposomes preparation. Their hydrodynamic diameter peak position was measured at 106 nm **(Figure 4.6)**. Here, the PEG polymer prevented the liposome aggregation process. Oku and co-workers found that PEGylated liposomes didn't aggregate when they were incubated in PBS at 37 °C for 30 min [70].

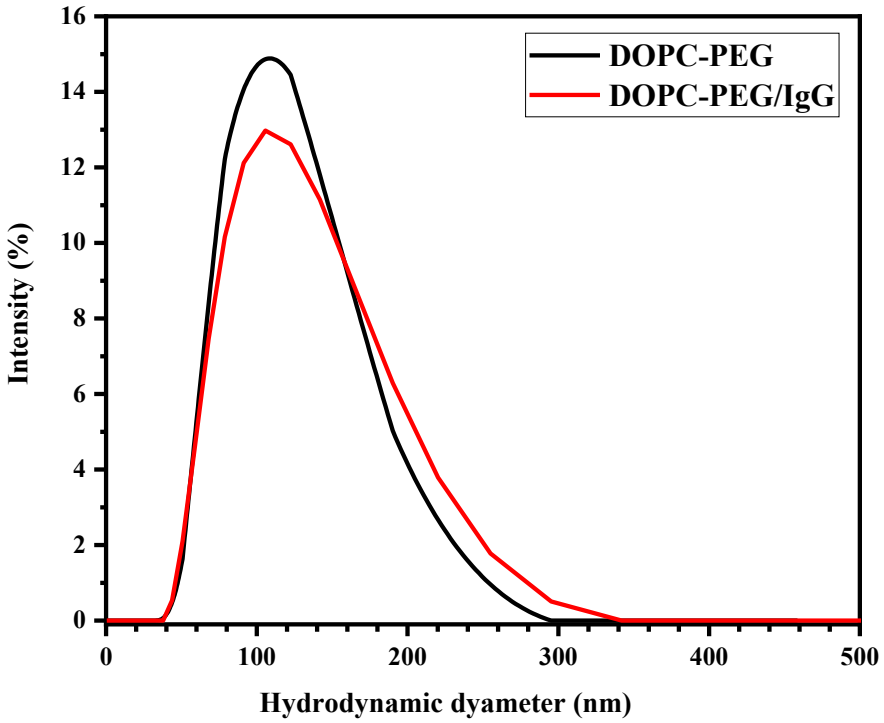

Figure 4.6: Hydrodynamic size distributions of bare DOPC-PEG liposomes (black) containing DOPC/DOPE-PEG in (1/0.01 mol/mol), and liposome/protein complex DOPC-PEG/IgG complex (red). Measurements were in PBS at 37 °C.

As shown in **(Table 4.3)**, upon incubation of DOPC-PEG with the IgG, neither particle size nor zeta potential distributions showed significant changes as indicated in **(Figure 4.6),** and **(Figure 4.7),** respectively. Hence the IgG was not adsorbed on the DOPC-PEG liposomal surface. This result was supported by Oku and co-workers finding. The researcher found that PEGylated liposomes did not aggregate when they were incubated with fetal bovine serum at 37 °C [70]. On the other hand; Caracciolo et al. 2014 found that PEGylated DOTAP liposomes incubated with HP were about 70 nm larger in size than bare liposomes. The authors suggest that the protein binding in PEGylated DOTAP was caused by the high PEG density used (10%) [6]. Many other studies showed that PE Gylation greatly reduces protein binding [6], [38], [47], [49]. This result can be explained by a large hydration shell formed by the PEG polymer preventing hydrophobic or electrostatic binding of proteins with the underlying NPs [47].

Table 4.3: **Average hydrodynamic diameter** (d), polydispersity index (PDI) and zeta potential (ξ) of pure DOPC-PEG liposomes and DOPC-PEG/IgG complex in PBS buffer at 20°C. (n=3) The individuals are listed in Appendix (**Table A.3)**.

DOPC-PEG	IgG	d (nm) ± sd	PDI± sd	ξ (mv) ± sd
+	-	117 ± 7	0.1 ±0.0	-5 ± 3
+	+	117 ± 7	0.3 ±0.0	-7 ± 5

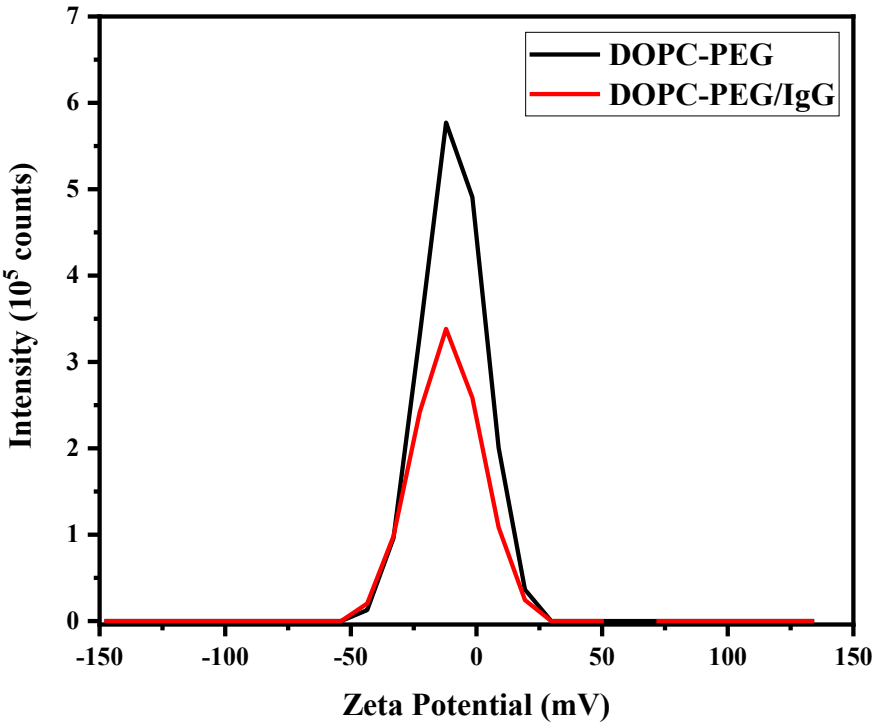

Figure 4.7: Top pane: zeta potential distributions of free IgG. Bottom panel: bare DOPC-PEG liposomes (black), and DOPC-PEG/IgG complex (red). Measurements were in PBS at 37 °C.

4.2 Fluorescence Spectroscopy

Fluorescence spectroscopy was used to investigate whether the interactions between the protein IgG and the three different liposome formulations involved conformational changes of the IgG structure. Proteins have three types of aromatic residues, which absorb UV light at nearly 280

nm: tryptophan (Trp), phenylalanine (Phe), and tyrosine (Tyr). The most intense absorption and emission among these three aromatic residues is the Trp, which has the higher molar absorption and intrinsic fluorescence quantum yield [71].

IgG contain 26 tryptophan residues [64]. The IgG possesses intrinsic fluorescence (tryptophan unit) in the ultraviolet spectral region. Several spectra of IgG, and liposome/IgG complexes emission were recorded. A spectrum of either PBS or a liposome dispersion (Appendix **Figure A.1- A.4**) were subtracted from IgG emission, to eliminate effects of scattering, and background. **(Figure 4.8)** show the absorption and emission of IgG solution.

Fluorescence quenching of a substance interacting with another molecule, added in increasing amounts as quenchers, can be used to measure the binding affinities between macromolecules and ligands acting. In fluorescence, quenching is defined as a decrease in quantum yield induced by molecular interactions [71].

Free IgG: In good agreement with literature values [64], free IgG in PBS (2.5 mg/ml) yielded an excitation maximum at 283 nm. Upon interaction between the Trps and solvent molecules, the energy of surface Trps decrease, thus Trps emit at longer wavelengths at around 350 nm[52]. Here the emission maximum was measured at 343 nm due to its highly polar environment and solvent accessibility.

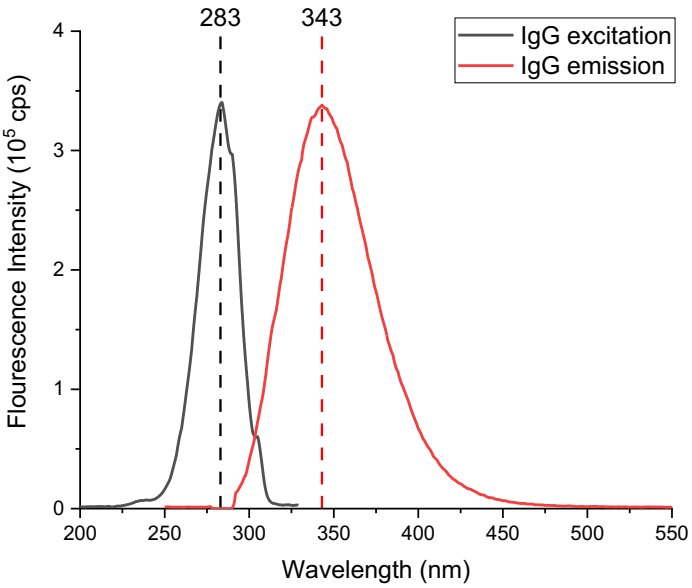

Figure 4.8: Absorption and emission spectra of IgG (2.5 mg/ml) measured in PBS at pH 7.40.

FL/IgG Complexes; As shown in (**Figure 4.9)**, the fluorescence emission spectra of Trp residues of IgG were quenched by the titration of FL. Increasing FL concentrations resulted in a reduction in the fluorescence emission intensity maximum of IgG, indicating a type of binding. Weissmann et al. 1974 incubated IgG with cationic liposomes. He found that cationic liposomes bind about 50% of the native protein [22]. Many other studies show IgG binding to cationic liposomes upon incubating with HP [5], [6], [51]. According to our finding, it can be assumed that FL is located near the Trp residues. Trp residues on the surface of the IgG are highly accessible to the solvent.

Thus, we assume that only the Trp residues on the IgG surface are quenched by the FL. The IgG emission wavelength didn't change significantly exhibiting a value of 343 nm (s.d. 1nm). Hence the IgG is not penetrating in the FL lipid membrane.

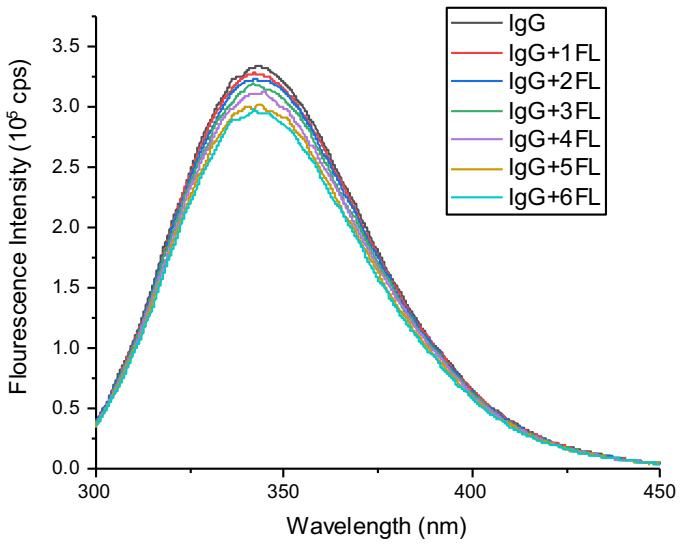

Figure 4.9: Fluorescence emission spectra of internal tryptophan residue of IgG and its fluorescence quenching by addition of FL in buffer solution (pH 7.40, T=310K, $\lambda_{ex} = 283\ nm$). The black line refers to the emission spectrum of 0.5 μM free IgG, while the numbers of FL added to IgG correspond to the emission spectrum after consecutive additions of 4 μl of FL at a concentration of 5.2 μM (injection numbers, concentration range from 5.2 μM to 31 μM). See (**Figure 3.8**).

DOPC/ IgG, and DOPC-PEG/ IgG Complexes; upon titration of DOPC **(Figure 4.10)**, and DOPC-PEG **(Figure 4.11)** to the IgG solution the maximum fluorescence intensity of IgG remained unchanged. This indicates that the IgG is not binding neither to DOPC nor to DOPC-PEG liposomes. Hence the lipids composition and surface charge highly influence the IgG binding to the nanoparticles. A study by Giulimondi et al. 2020 concluded that no binding occurred when DOPC liposomes were incubated with HP at increasing concentrations of HP [5]. Sangrà et al. 2017 studied the interaction between BSA and LUV of Neutral and pegylated-PC with 20% cholesterol using fluorescence quenching. The quenching effect was observed in both cases [49]. The addition of cholesterol greatly enhanced the presence of H-bond interactions between BSA and liposomes, explaining this result [22]. Caracciolo et al. 2014 found IgG ca. 15% RPA adhered on PEGylated liposomal surfaces upon incubated with HP. Here the IgG binding was due to high PEG density added (10%) [6].

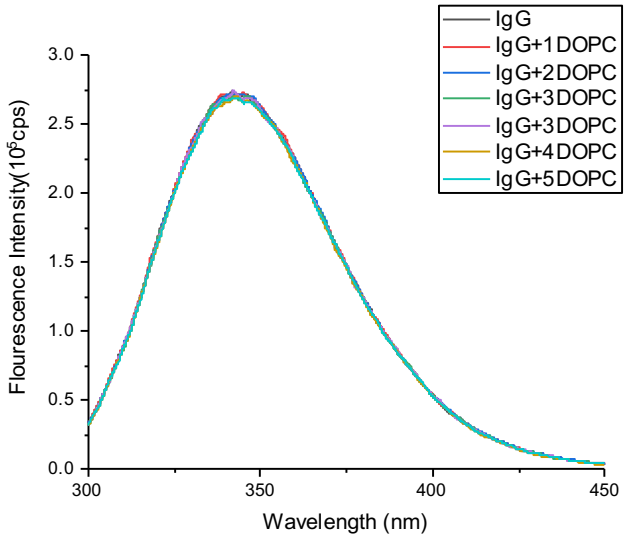

Figure 4.10: Fluorescence emission spectra upon incubation of IgG with DOPC, in buffer solution (pH 7.40, T=310K, $\lambda_{ex} = 283\ nm$). The black line refers to the emission spectrum of 0.5 μM free IgG while the numbers of DOPC added to IgG correspond to the emission spectrum after consecutive additions of 4 μl DOPC at a concentration of 5.1 μM (injection numbers, concentration range from 5.1 μM to 30.6 μM), see (**Figure 3.8**).

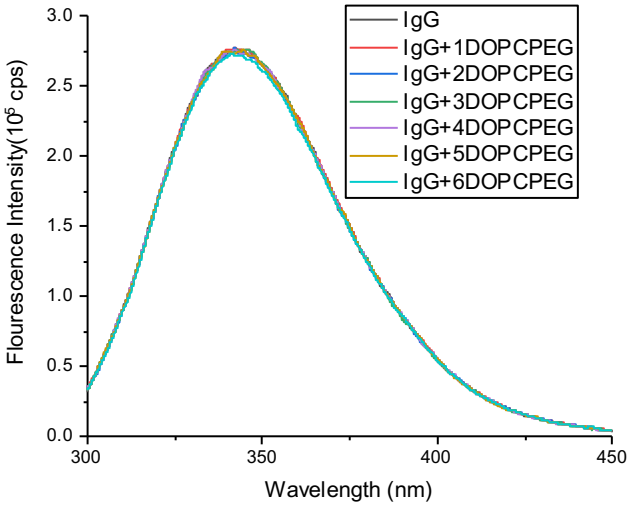

Figure 4.11: Fluorescence emission spectra upon incubation of IgG with DOPC-PEG in buffer solution (pH 7.40, T=310K, $\lambda_{ex} = 283\ nm$). The black line refers to the emission spectrum of 0.5 μM free IgG while the numbers of DOPC-PEG added to IgG correspond to the emission spectrum after consecutive additions of 4 μl DOPC-PEG at a concentration of 4.2 μM (injection numbers, concentration range from 5.1 μM to 25.2 μM), see (**Figure 3.8**).

Fluorescence Quenching Constant of FL/IgG Complexes (k_{sv}); by applying the emission intensity of tryptophan residue of IgG at 343 nm to Stern-Volmer equation **(Equation 5),** Stern-Volmer quenching constant and the quenching rate constant can be obtained, which provide an indication about the quenching mechanism.

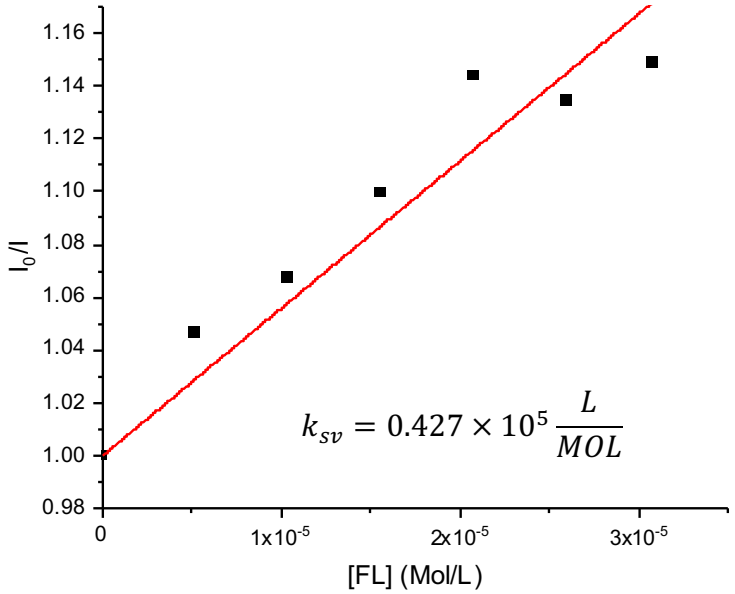

Figure 4.12: Stern-Volmer plot of fluorescence quenching of IgG by FL at 310K, and Stern-Volumer quenching constant.

There are two types of fluorescence quenching: dynamic or collisional quenching and static quenching. Dynamic quenching occurs when the fluorophore and quencher diffuse in the excited state, following the fluorophore returns to the ground state without emitting a photon. Conversely, static quenching takes place when the fluorophore and the quencher molecules form a non-fluorescent complex in the ground state. Static and dynamic quenching require molecular contact between the fluorophore and the quencher and can be distinguished by Stern-Volumer plot. A straight line corresponds to dynamic quenching while static quenching can be characterized by upward deviation [49]. Thus, in our study the quenching is dynamic.

The linear Stern-Volmer plot indicate a single class of fluorophores (tryptophan) in protein quenched by charged quenchers [49], [62]. Since the curvature in the plot usually indicates that dynamic and static quenching coexist or that some emitters are inaccessible to quencher molecules [52].

Here (**Figure 4.12**), IgG is quenched only by surface-exposed tryptophan residues. Thus, the lifetime τ_0 in this study is referred only to surface Trp residues (3.6 ns) [52], which have the longest lifetimes among the buried and partially buried Trps. The bimolecular quenching constant K_q have a limit value near 1×10^{10} L/mol×s **(Table 4.4)**. A value larger than the diffusion-controlled limit indicates some binding interaction [62].

Table 4.4: Average $K_{SV\ and}$ K_q values of fluorescence quenching of IgG by FL at 310 K. Values are shown as mean ± standers deviation of three replicates.

T(K)	K_{SV} (L/mol)	K_q (L/mol×s)
310	4272.35 ± 880.1	1.2×10^{12}

Binding Constant of FL/IgG Complexes (k_a); modified Stern-Volmer equation can be used to further analyse the fluorescence data by applying (**Equation 6)**. The modified Stern-Volmer binding constant can be calculated to analyse if the interaction between IgG and FL is strong, moderate, or weak.

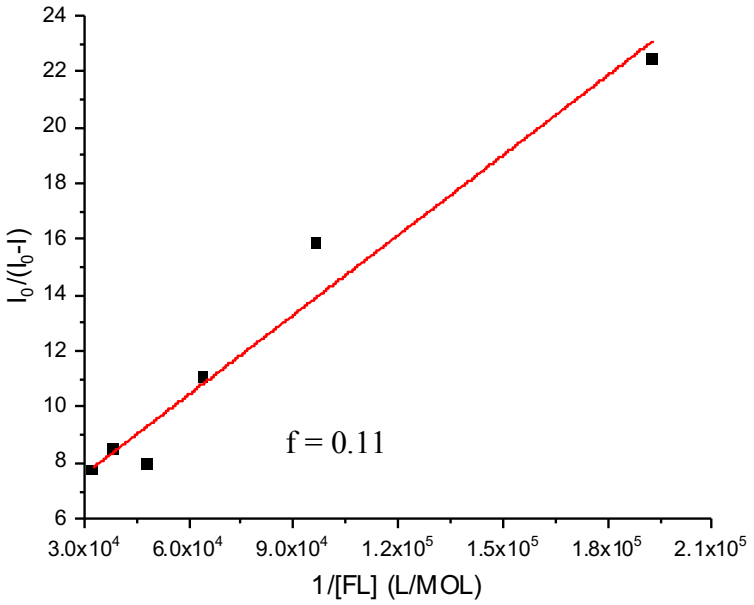

Figure 4.13: Modified Stern-Volmer plot of IgG quenching by FL at 310K, and the inaccessible fraction f.

The value of K_a was found in the order of 10^5 L/mol **(Table 4.5).** Chaves and co-workers studied the binding of pheophytin with human serum albumin (HSA) using fluorescence quenching at 310 K. The value of K_a was $5.95 \times 10^4\ L/mol$. They concluded that HSA can carry the pheophytin and they have moderate interactions [71]. Due to large standard deviation in K_a, further research could provide more precise results.

The inaccessible fraction (f) value indicates that only 11% of the emission quenched by FL **(Table 4.5)**. As a result, Trp residues in IgG are not equally fluorescent, and only surface Trp residues quenched by FL. A small value of f, and the linear regression in the modified Stern-Volmer plot (**Figure 4.13**) without deviation provide that the binding of Trp residues to FL doesn't cause a conformational change in the IgG. Since conformational changes in proteins can expose shielded Trp residues to solvent molecules, which indicated by a large value of f [62].

Table 4.5: Average Ka value of the fluorescence quenching of the IgG by FL at 310 K. Values are shown as mean ± standers deviation of three replicates.

T(K)	K_a(L/mol)	f
310	$1.5 \pm 1.8 \times 10^5$	0.11 ± 0.06

Binding Constant and Binding Site of FL/IgG Complexes; the number of binding sites on the IgG can be calculated by applying (**Equation (8)).** From the plot below (**Figure 4.14**) ≈ 1 , which indicates that during the interaction IgG contains only one binding site for FL. A majority of ligands binds to proteins reversibly and exhibit moderate affinity [binding constants: $(1 - 15) \times 10^4$L/mol] [63]. In **(Table 4.6)** the large standard deviation of K reveled that more experiments need to be conducted to obtain more accurate results.

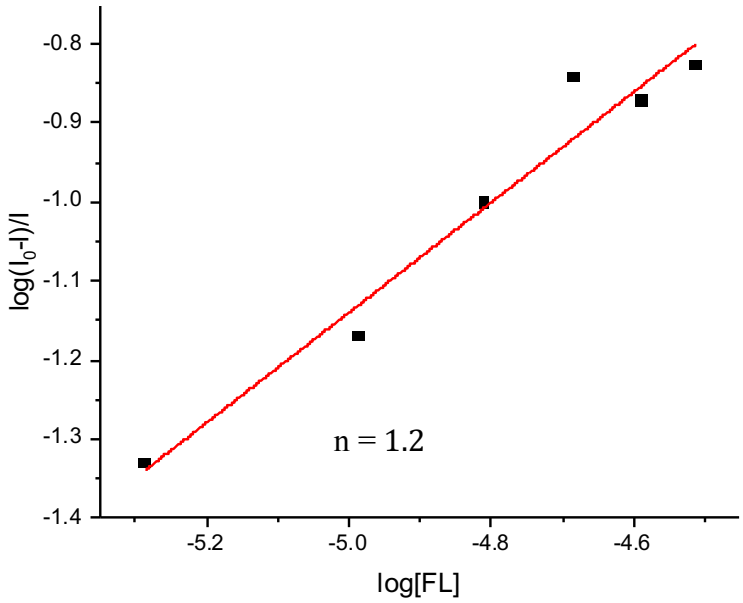

Figure 4.14: Binding site and binding constant of the fluorescence quenching of the IgG by FL at 310K.

Table 4.6: Average number of binding site and binding constant of IgG-FL complex, errors are mean ± standers deviation of three replicates.

T(K)	K(L/mol)	n
310	$1.0 \pm 1.8 \times 10^5$	1.2 ± 1.1

4.3 Isothermal Titration Calorimetry (ITC)

Isothermal titration calorimetry (ITC) provides insight into the thermodynamics of biomolecular interaction, including binding enthalpy (ΔH), entropy (ΔS), free energy (ΔG), binding constant (K_a), and stoichiometry (N). Here, the investigation of thermodynamic profile of the interaction between IgG and liposomes is important to understand the molecular recognition nature [17]. Due to high concentration required by the instrument, and the high cost of the IgG, each measurement was carried out only once. During experiments, the antibody IgG was titrated into FL, DOPC or DOPC-PEG liposomes, and the power, needed to compensate the energy, produced or used during the reaction, was measured. The measured curves were compensated by the IgG dilution`s and liposome´s dilution curves recorded previously, and the reaction enthalpy vs. molecular ratio of IgG to lipids were plotted to calculate the reaction enthalpy (ΔH), entropy (ΔS), and stoichiometry (N).

FL /IgG Complexes; IgG solution at a concentration of $1.35\mu M$ was titrated into FL at $0.15\ mM$ concentration. As shown in **(Figure 4.15)**, the experiment yielded titration patterns with both exothermic and endothermic energy contributions **(Figure 4.15 Upper panel**). Anbazhagan et al. 2011obtained similar result when titrated Bovine plasma protein (PDC-109) in to DMPC. The titration exhibited a complex pattern of endothermic and exothermic energy contributions in the liquid crystalline phase of DMPC [72].

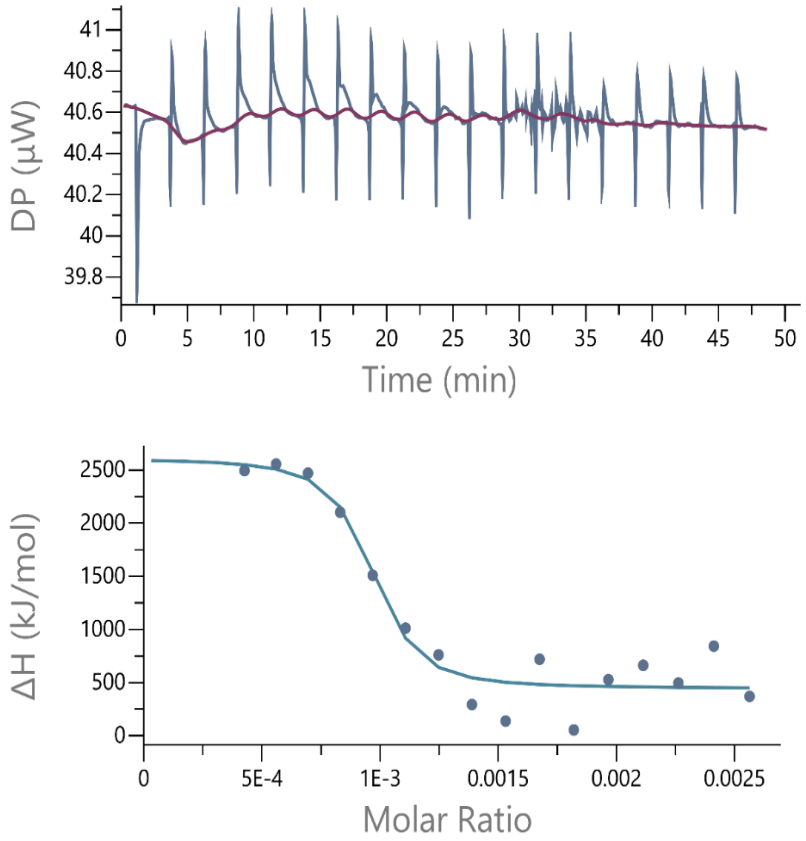

Figure 4.15: ITC titration for the binding of IgG (1.35 μM) to FL (0.15 mM) at room temperature. Upper panel represents the raw data of titration, power change as a series of automatic injection (4 μl each) vs. time. The bottom panel shows the integrated enthalpy of binding obtained from raw data, after subtracting the dilution enthalpies vs. molar ratio of IgG to FL showing experimental (•) and the best fit (-).

Hence the reference titrations (IgG-in-buffer and buffer-in-liposome) were both exothermic, the reaction enthalpy of IgG with FL remained endothermic after baseline correction (**Figure 4.15 Bottom panel**). The calculated binding affinity (K_D) of 0.94 nM (s.d. 0.85 nM) (**Table 4.7)** indicated a rather weak binding between the two partners as well as the very small number of binding site (N) of 9.1×10^{-4} (s.d. 4.1×10^{-5}).

It has been found that the binding of IgG to FL was endothermic in nature and was governed by a positive entropic contribution. Considering that the enthalpy as well as entropy values were favorable **(Figure 4.16)**, hydrophobic and van der Waals interactions may dominate the binding

[63], [3]. Lin et al. 2007 found that hydrophobic force dominates the interaction between the beta-amyloid peptide β-amyloid (A β) and zwitterionic lipids, while electrostatic and hydrophobic forces are responsible for the interaction between A β and charged liposomes [73]. Many studies have reported endothermic binding (entropically favored) of proteins and peptides to lipid membranes [72]-[75]. However, it should be considered, that protein denaturation is also an endothermic and entropy driven process. Therefore, IgG denaturation in the presence of FL has to be further investigated using additional methods.

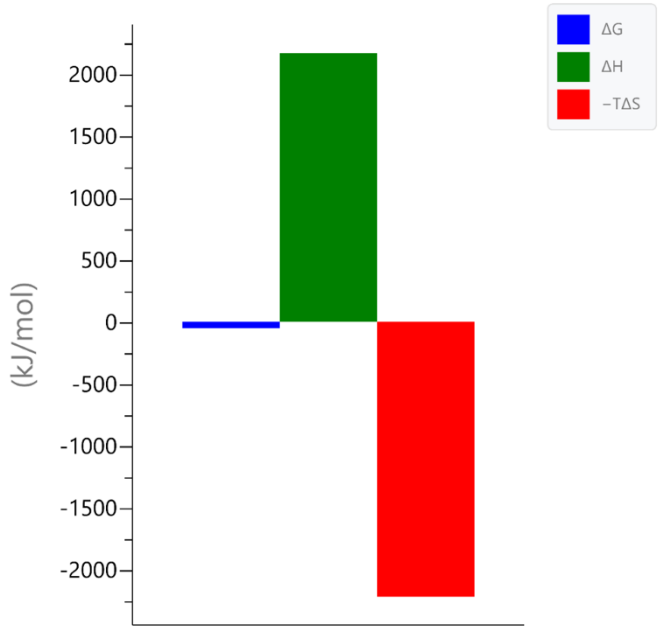

Figure 4.16: Thermodynamic characteristics of IgG/FL interaction at RT. ΔH (green), $-T\Delta S$ (red), and ΔG (blue).

Table 4.7: The thermodynamic parameters for NPs/IgG complexes using ITC at RT.

Complexes	**ΔH (KJ/mol)**	**ΔS (KJ/mol K)**	**ΔG (KJ/mol)**	**N (10^{-3}Sites)**	**K_d (nM)**
FL/IgG	2170 ± 238	7.2	-51.6	0.91 ± 0.04	0.94 ± 0.85
DOPC/IgG	-	-	-	-	-
DOPC-PEG/IgG	-1480	- 4.7	-30.8	0.001	4000

DOPC/IgG Complexes; IgG solution at a concentration of 1.35 μM was titrated into DOPC liposomes at 0.15 mM concentration similar to previous experiments using FL. As shown in (**Figure 4.17)**, the experiment yielded titration patterns with pure exothermic signals (**Figure 4.17 Upper panel**). After baseline correction with IgG and liposomes dilutions, the IgG-DOPC titration did not shown any characteristic binding pattern (**Figure 4.17 Bottom panel**) indicating no interaction between DOPC and IgG.

This result was in good agreement with our findings in DLS **(Figure 4.4)**, ELS **(Figure 4.5)**, and fluorescence spectroscopy **(Figure 4.10)** experiments. Sangrà et al. 2017 achieved similar result, when injected BSA in to LUV of PC: CHOL (20%).The experiment yielded titration patterns with endothermic energy contributions but didn't reveal any changes in enthalpy upon the addition of BSA, hence no binding was observed [49].

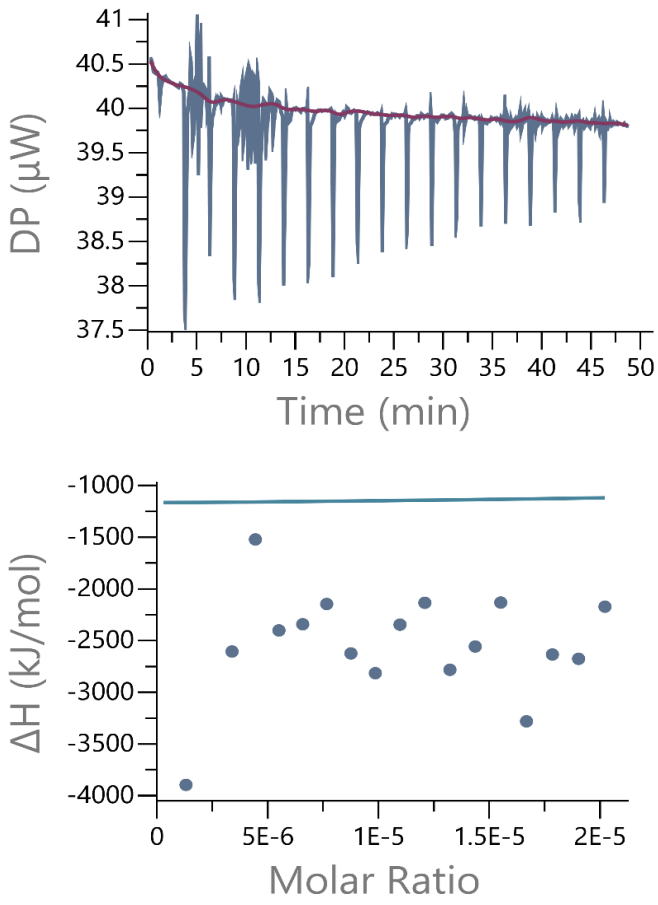

Figure 4.17: ITC titration of IgG (1.35 μM) into DOPC liposomes (0.15 mM) at room temperature. Upper panel represents the change in power as a series of automatic injection (4 μl each) vs. time. The bottom panel indicates the integrated enthalpy in each injection after correction with IgG and FL dilution enthalpies vs. molar ratio of IgG to FL showing experimental (•) and the best fit (-).

DOPC-PEG/IgG Complexes; To determine the thermodynamic characteristics of the IgG/DOPC-PEG binding, IgG solution at 1.35 µM was titrated into a DOPC-PEG dispersion at 12.50 mM concentration. The elevated lipid concentration was necessary to record at least a part of the binding curve. The experiment resulted titration patterns with pure exothermic contributions **(Figure 4.18)**. After baseline subtraction of the dilution curves, the binding enthalpy remained exothermic. The calculated number of binding site (N) was ca. 1×10^{-6}. However, this value is very low, it has to be considered that the first part of the curve was missing, therefore an exact determination of N was not possible. The calculated binding affinity

(K_D) was (4 μM) that is higher than that obtained for FL/IgG interaction (0.94 nM) **(Table 4.7)**. Due to the missing part of the titration curve, the error of K_D, calculated from the slope of the titration curve, was very high. Comparing this result with the findings of DLS (**Figure 4.6**), ELS, **(Figure 4.7)**, and fluorescence spectroscopy **(Figure 4.11)** experiments, showing no interaction between IgG and DOPE-PEG, the contradiction is obvious. Consequently, the experiment has to be repeated in the future for more precise results. This result is further contradicting to Sangrà et al. 2017 finding. He injected BSA in to LUV of PC: CHOL (20%): PEG (3%). The experiment yielded titration patterns with endothermic energy contributions and indicated that the heat difference was not enough to determine thermodynamic parameters, hence no binding was observed [49]. **Prozeller et al. 2020** found that IgG undergo more hydrophobic interactions upon titrated with PEGylated PS-NPs. while hydrophilic interactions i.e. electrostatic interactions take place titrations for the functionalized PEGylated-NPs [3].

Without consideration of the absolute values of the thermodynamic parameters, the exothermic characteristics of the reaction enthalpy ($-\Delta H$) indicated the formation of hydrogen bonds (**Figure 4.19)** during the interaction while the entropy loss ($-\Delta S$) indicated unfavorable conformational changes.

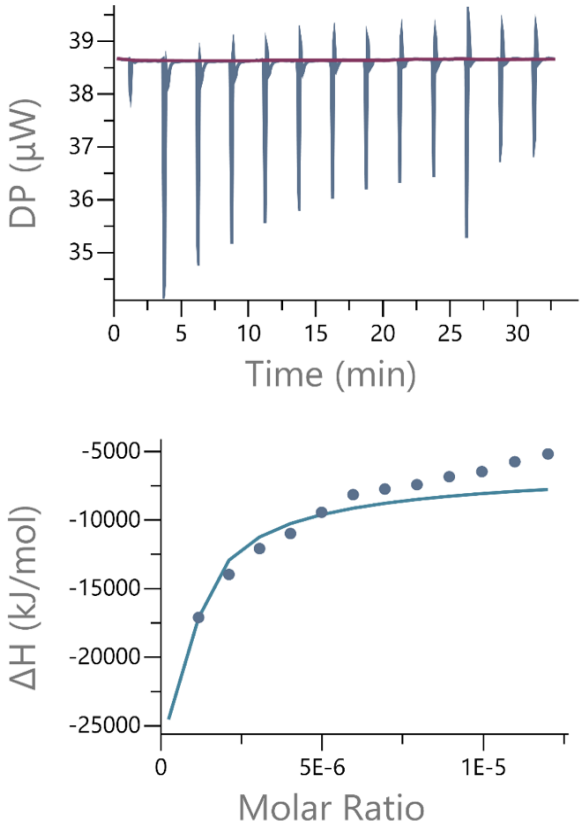

Figure 4.18: ITC titration of IgG (1.35 μM) into DOPC-*PEG* liposomes (12.5 mM) at room temperature. Upper panel represents the change in power as a series of automatic injection (4 μl each) vs. time. The bottom panel indicates the integrated enthalpy in each injection after correction with IgG and FL dilution enthalpies vs. molar ratio of IgG to FL showing experimental (•) and the best fit (-).

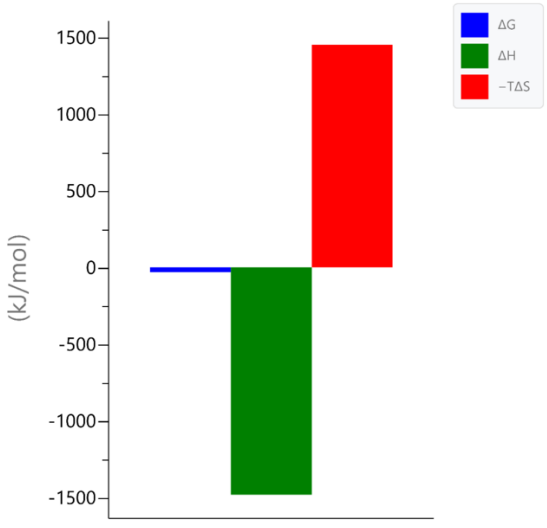

Figure 4.19: Thermodynamic characteristics of IgG/DOPC-PEG interaction at RT. ΔH (green), $-T\Delta S$ (red), and ΔG (blue).

Chapter 5: Conclusion

Since IgG was involved in the corona formation on FL surface [51]. Here, the interactions between human immunoglobulin (IgG) with positively charged fusogenic (FL), neutral (DOPC) and PEGylated (DOPC-PEG) liposomes have been studied in details using DLS, ELS, fluorescence, and ITC techniques.

Based on zeta potential and DLS measurements, IgG adsorption on FL surface caused a significant increase in hydrodynamic diameters, while the zeta potential indicated neutral charge distribution similar to that of pure IgG, indicating a dense protein layer on the FL surface. The force that drives the IgG/FL interaction is of an electrostatic nature. Both DOPC and DOPC-PEG showed similar liposomal sizes and zeta potentials as bare liposomes, thus IgG is not present on either surface.

Fluorescence spectroscopy was used to investigate the stability of IgG when interacting with different liposomal formulations. Trp residues are randomly distributed within IgG molecules, and their contributions to fluorescence emission are unequal. Here, we examined Trps with fluorescence quenching. In FL titrations, only the surface-exposed tryptophan residues showed quenching without a shift in emission wavelength, indicating that the IgG does not involve in the lipid membranes of FL. Regarding DOPC and DOPC-PEG, the maximum fluorescence intensity of IgG remained unchanged. The fluorescence date for the IgG/FL complexes was further analyzed. The association constant value ($K_a \approx 10^5$ L·mol^{-1}) indicate a moderate IgG/FL interaction. The bimolecular quenching constant (K_q) values in the order of 10^{12} L·mol^{-1}·s^{-1} indicate the absence of static fluorescence. According to the binding sites≈ 1, IgG contains only one binding site for FL during the interaction.

Moreover, to obtain the thermodynamic profile of IgG/liposome complexes, and to better understand the molecular recognition nature by antibodies, isothermal titration calorimetry was conducted once for each liposome/IgG complex due to the high concentration required by the instrument and the high cost of the IgG. According to the thermodynamic parameters of FL, the

spontaneous interaction is endothermic ($\Delta H > 0$), and hydrophobic effects dominate the binding ($\Delta S > 0$). In the case of DOPC, we found no evidence of IgG/DOPC binding, consistent with DLS, ELS, and fluorescence findings. Regarding the DOPC-PEG, which exhibits a contradictory result in non-covalent bonds being formed during its interaction with the IgG ($\Delta H < 0$). Here, future studies could elucidate whether we have a binding or not.

These results indicate that FL is a promising drug carrier. Future studies could elucidate how the IgG binds to fusogenic liposomes e.g FTIR, DSC...etc. The ITC experiments should be repeated for more precise results since we had one experiment per each IgG/NPs complex. Furthermore, liposome formulations can be incubated with plasma samples, and measure the hydrodynamic diameter and zeta potential once again, to analyze the composition of the forming protein corona, and in particular to identify the adsorption of IgG on NPs.

Outlook

In this work, measurement techniques have been established to determine the binding affinity of blood serum proteins to liposomal surfaces with different chemical characteristics. Because establishment processes are very time-consuming, an adequate number of measurements repetition couldn´t be performed during the available time period. Therefore, liposomal preparation and affinity measurements have to be repeated to verify the results published in this work.

However, the protein IgG used in this study showed moderate binding to FLs. This effect has to be compared to other serum proteins to estimate its biological relevance. As presented in our preliminary mass spectroscopic study, other serum proteins, such as apolipoproteins (A1, C3, C4, and E) or vitronectin, bind more efficiently to FLs than IgG showing more presence on the liposome surface. Therefore, we hypothesize that those proteins also show higher kSV values than IgG. Our hypothesis has to be validated based on further fluorescence quenching analysis.

FLs are going to be used in vivo as drug delivery vehicles injected into the bloodstream. Based on our affinity analysis with some of the main blood serum proteins, among others IgG and apolipoproteins, the possible immune response can be estimated. If necessary, the liposomal composition can be adjusted to change the biological identity of the drug carriers and correspondingly to reduce IgG affinity and the particle blood clearance.

References

[1] S. Kube *et al.*, 'Fusogenic Liposomes as Nanocarriers for the Delivery of Intracellular Proteins', *Langmuir*, vol. 33, no. 4, pp. 1051–1059, Jan. 2017, doi: 10.1021/ACS.LANGMUIR.6B04304.

[2] M. Hoffmann, N. Hersch, R. Merkel, A. Csiszar, and B. Hoffmann, 'Changing the Way of Entrance: Highly Efficient Transfer of mRNA and siRNA via Fusogenic Nano-Carriers', *J Biomed Nanotechnol*, vol. 15, no. 1, pp. 170–183, Jan. 2019, doi: 10.1166/JBN.2019.2663.

[3] D. Prozeller, C. Rosenauer, S. Morsbach, and K. Landfester, 'Immunoglobulins on the surface of differently charged polymer nanoparticles', *Biointerphases*, vol. 15, no. 3, p. 031009, May 2020, doi: 10.1116/6.0000139.

[4] A. Csiszár, N. Hersch, S. Dieluweit, R. Biehl, R. Merkel, and B. Hoffmann, 'Novel fusogenic liposomes for fluorescent cell labeling and membrane modification', *Bioconjug Chem*, vol. 21, no. 3, pp. 537–543, Mar. 2010, doi: 10.1021/BC900470Y.

[5] F. Giulimondi *et al.*, 'Author Correction: Interplay of protein corona and immune cells controls blood residency of liposomes', *Nat Commun*, vol. 11, no. 1, Dec. 2020, doi: 10.1038/S41467-020-15500-9.

[6] G. Caracciolo *et al.*, 'The liposome–protein corona in mice and humans and its implications for in vivo delivery', *J Mater Chem B*, vol. 2, no. 42, pp. 7419–7428, Oct. 2014, doi: 10.1039/C4TB01316F.

[7] S. C. Semple, A. Chonn, and P. R. Cullis, 'Interactions of liposomes and lipid-based carrier systems with blood proteins: Relation to clearance behaviour in vivo', *Adv Drug Deliv Rev*, vol. 32, no. 1–2, pp. 3–17, Jun. 1998, doi: 10.1016/S0169-409X(97)00128-2.

[8] A. Torcello-Gómez *et al.*, 'Adsorption of antibody onto Pluronic F68-covered nanoparticles: link with surface properties', *Soft Matter*, vol. 7, no. 18, pp. 8450–8461, Sep. 2011, doi: 10.1039/C1SM05570D.

[9] R. Kolašinac, C. Kleusch, T. Braun, R. Merkel, and A. Csiszár, 'Deciphering the functional composition of fusogenic liposomes', *Int J Mol Sci*, vol. 19, no. 2, Feb. 2018, doi: 10.3390/IJMS19020346.

[10] G. Vidarsson, G. Dekkers, and T. Rispens, 'IgG subclasses and allotypes: from structure to effector functions', *Front Immunol*, vol. 5, no. OCT, 2014, doi: 10.3389/FIMMU.2014.00520.

[11] H. Sato, Y. Miyashita, K. Sasaki, A. Kishimura, T. Mori, and Y. Katayama, 'Non-covalent Coating of Liposome Surface with IgG through Its Constant Region', *https://doi.org/10.1246/cl.180181*, vol. 47, no. 6, pp. 770–772, Apr. 2018, doi: 10.1246/CL.180181.

[12] G. Caracciolo, 'Liposome-protein corona in a physiological environment: challenges and opportunities for targeted delivery of nanomedicines', *Nanomedicine*, vol. 11, no. 3, pp. 543–557, 2015, doi: 10.1016/J.NANO.2014.11.003.

[13] R. Pieper *et al.*, 'The human serum proteome: display of nearly 3700 chromatographically separated protein spots on two-dimensional electrophoresis gels and identification of 325 distinct proteins', *Proteomics*, vol. 3, no. 7, pp. 1345–1364, Jul. 2003, doi: 10.1002/PMIC.200300449.

[14] N. Onishchenko, D. Tretiakova, and E. Vodovozova, 'Spotlight on the protein corona of liposomes', *Acta Biomater*, vol. 134, pp. 57–78, Oct. 2021, doi: 10.1016/J.ACTBIO.2021.07.074.

[15] T. Kopac, 'Protein corona, understanding the nanoparticle-protein interactions and future perspectives: A critical review', *Int J Biol Macromol*, vol. 169, pp. 290–301, Feb. 2021, doi: 10.1016/J.IJBIOMAC.2020.12.108.

[16] S. W. de Taeye, T. Rispens, and G. Vidarsson, 'The ligands for human igG and their effector functions', *Antibodies*, vol. 8, no. 2. MDPI, Jun. 01, 2019. doi: 10.3390/antib8020030.

[17] V. Frasca, 'Biophysical characterization of antibodies with isothermal titration calorimetry', *J Appl Bioanal*, vol. 2, no. 3, pp. 90–102, Jul. 2016, doi: 10.17145/jab.16.013.

[18] D. Pozzi *et al.*, 'Surface chemistry and serum type both determine the nanoparticle-protein corona', *J Proteomics*, vol. 119, pp. 209–217, Apr. 2015, doi: 10.1016/J.JPROT.2015.02.009.

[19] J. M. Reichert, 'Antibody Fc: Linking Adaptive and Innate Immunity: Editors Margaret E. Ackerman, Falk Nimmerjahn', *MAbs*, vol. 6, no. 3, p. 619, May 2014, doi: 10.4161/MABS.28617.

[20] V. Raúl, G. Román, J. C. Murray, and L. M. Weiner, 'Antibody-Dependent Cellular Cytotoxicity (ADCC) BRIEF HISTORY OF ADCC', 2012.

[21] A. W. P. Vermeer, W. Norde, and A. van Amerongen, 'The Unfolding/Denaturation of Immunogammaglobulin of Isotype 2b and its Fab and Fc Fragments', *Biophys J*, vol. 79, no. 4, pp. 2150–2154, Oct. 2000, doi: 10.1016/S0006-3495(00)76462-9.

[22] G. Weissmann, A. Brand, and E. C. Franklin, 'Interaction of immunoglobulins with liposomes', *J Clin Invest*, vol. 53, no. 2, pp. 536–543, 1974, doi: 10.1172/JCI107587.

[23] M. Kiyoshi *et al.*, 'Structural basis for binding of human IgG1 to its high-affinity human receptor FcγRI', *Nat Commun*, vol. 6, Apr. 2015, doi: 10.1038/NCOMMS7866.

[24] V. Irani, A. J. Guy, D. Andrew, J. G. Beeson, P. A. Ramsland, and J. S. Richards, 'Molecular properties of human IgG subclasses and their implications for designing therapeutic monoclonal antibodies against infectious diseases', *Mol Immunol*, vol. 67, no. 2 Pt A, pp. 171–182, Oct. 2015, doi: 10.1016/J.MOLIMM.2015.03.255.

[25] A. D. Bangham and R. W. Horne, 'NEGATIVE STAINING OF PHOSPHOLIPIDS AND THEIR STRUCTURAL MODIFICATION BY SURFACE-ACTIVE AGENTS

AS OBSERVED IN THE ELECTRON MICROSCOPE', *J Mol Biol*, vol. 8, no. 5, pp. 660–668, 1964, doi: 10.1016/S0022-2836(64)80115-7.

[26] F. U. Din *et al.*, 'Effective use of nanocarriers as drug delivery systems for the treatment of selected tumors', *Int J Nanomedicine*, vol. 12, pp. 7291–7309, Oct. 2017, doi: 10.2147/IJN.S146315.

[27] C. Horejs, 'From lipids to lipid nanoparticles to mRNA vaccines', *Nat Rev Mater*, vol. 6, no. 12, pp. 1075–1076, Dec. 2021, doi: 10.1038/S41578-021-00379-9.

[28] T. Wiedenhoeft *et al.*, 'The Basement Membrane in a 3D Breast Acini Model Modulates Delivery and Anti-Proliferative Effects of Liposomal Anthracyclines', *Pharmaceuticals (Basel)*, vol. 13, no. 9, pp. 1–17, Sep. 2020, doi: 10.3390/PH13090256.

[29] S. J. Singer and G. L. Nicolson, 'The fluid mosaic model of the structure of cell membranes', *Science*, vol. 175, no. 4023, pp. 720–731, 1972, doi: 10.1126/SCIENCE.175.4023.720.

[30] U. B. Kompella, R. S. Kadam, and V. H. L. Lee, 'Recent advances in ophthalmic drug delivery', *Ther Deliv*, vol. 1, no. 3, p. 435, Sep. 2010, doi: 10.4155/TDE.10.40.

[31] N. Oku *et al.*, 'Effect of serum protein binding on real-time trafficking of liposomes with different charges analyzed by positron emission tomography', *Biochim Biophys Acta*, vol. 1280, no. 1, pp. 149–154, Apr. 1996, doi: 10.1016/0005-2736(95)00283-9.

[32] A. Akinc *et al.*, 'The Onpattro story and the clinical translation of nanomedicines containing nucleic acid-based drugs', *Nat Nanotechnol*, vol. 14, no. 12, pp. 1084–1087, Dec. 2019, doi: 10.1038/S41565-019-0591-Y.

[33] Š. Koudelka *et al.*, 'Liposomes with high encapsulation capacity for paclitaxel: Preparation, characterisation and in vivo anticancer effect', *J Pharm Sci*, vol. 99, no. 5, pp. 2309–2319, 2010, doi: 10.1002/JPS.21992.

[34] R. Kunstfeld *et al.*, 'Paclitaxel encapsulated in cationic liposomes diminishes tumor angiogenesis and melanoma growth in a "humanized" SCID mouse model', *J Invest Dermatol*, vol. 120, no. 3, pp. 476–482, Mar. 2003, doi: 10.1046/J.1523-1747.2003.12057.X.

[35] K. Yang, B. Mesquita, P. Horvatovich, and A. Salvati, 'Tuning liposome composition to modulate corona formation in human serum and cellular uptake', *Acta Biomater*, vol. 106, pp. 314–327, Apr. 2020, doi: 10.1016/J.ACTBIO.2020.02.018.

[36] X. Yan, G. L. Scherphof, and J. A. A. M. Kamps, 'Liposome opsonization', *J Liposome Res*, vol. 15, no. 1–2, pp. 109–139, 2005, doi: 10.1081/LPR-64971.

[37] J. Milton Harris and R. B. Chess, 'Effect of pegylation on pharmaceuticals', *Nat Rev Drug Discov*, vol. 2, no. 3, pp. 214–221, Mar. 2003, doi: 10.1038/NRD1033.

[38] L. Hong, Z. Wang, X. Wei, J. Shi, and C. Li, 'Antibodies against polyethylene glycol in human blood: A literature review', *J Pharmacol Toxicol Methods*, vol. 102, Mar. 2020, doi: 10.1016/J.VASCN.2020.106678.

[39] K. Maruyama, A. Okamoto, M. Iwatsuru, T. Yuda, C. Ishikura, and S. Kojima, 'Effect of molecular weight in amphipathic polyethyleneglycol on prolonging the circulation time

of large unilamellar liposomes', *Chem Pharm Bull (Tokyo)*, vol. 39, no. 6, pp. 1620–1622, 1991, doi: 10.1248/CPB.39.1620.

[40] J. D. Chalmers, J. van Ingen, R. van der Laan, and J. L. Herrmann, 'Liposomal drug delivery to manage nontuberculous mycobacterial pulmonary disease and other chronic lung infections', *Eur Respir Rev*, vol. 30, no. 161, Sep. 2021, doi: 10.1183/16000617.0010-2021.

[41] S. Kube *et al.*, 'Fusogenic Liposomes as Nanocarriers for the Delivery of Intracellular Proteins', *Langmuir*, vol. 33, no. 4, pp. 1051–1059, Jan. 2017, doi: 10.1021/ACS.LANGMUIR.6B04304.

[42] A. Csiszár *et al.*, 'Resveratrol encapsulated in novel fusogenic liposomes activates Nrf2 and attenuates oxidative stress in cerebromicrovascular endothelial cells from aged rats', *J Gerontol A Biol Sci Med Sci*, vol. 70, no. 3, pp. 303–313, Mar. 2015, doi: 10.1093/GERONA/GLU029.

[43] A. Csiszár *et al.*, 'Resveratrol Encapsulated in Novel Fusogenic Liposomes Activates Nrf2 and Attenuates Oxidative Stress in Cerebromicrovascular Endothelial Cells From Aged Rats', *J Gerontol A Biol Sci Med Sci*, vol. 70, no. 3, p. 303, Mar. 2015, doi: 10.1093/GERONA/GLU029.

[44] D. Baimanov, R. Cai, and C. Chen, 'Understanding the Chemical Nature of Nanoparticle-Protein Interactions', *Bioconjug Chem*, vol. 30, no. 7, pp. 1923–1937, Jun. 2019, doi: 10.1021/ACS.BIOCONJCHEM.9B00348.

[45] T. M. Göppert and R. H. Müller, 'Adsorption kinetics of plasma proteins on solid lipid nanoparticles for drug targeting', *Int J Pharm*, vol. 302, no. 1–2, pp. 172–186, Sep. 2005, doi: 10.1016/J.IJPHARM.2005.06.025.

[46] K. Nienhaus, H. Wang, and G. U. Nienhaus, 'Nanoparticles for biomedical applications: exploring and exploiting molecular interactions at the nano-bio interface', *Mater Today Adv*, vol. 5, p. 100036, Mar. 2020, doi: 10.1016/J.MTADV.2019.100036.

[47] Q. Yang and S. K. Lai, 'Anti-PEG immunity: emergence, characteristics, and unaddressed questions', *Wiley Interdiscip Rev Nanomed Nanobiotechnol*, vol. 7, no. 5, pp. 655–677, Sep. 2015, doi: 10.1002/WNAN.1339.

[48] J. T. Huckaby *et al.*, 'Structure of an anti-PEG antibody reveals an open ring that captures highly flexible PEG polymers', *Communications Chemistry 2020 3:1*, vol. 3, no. 1, pp. 1–8, Sep. 2020, doi: 10.1038/s42004-020-00369-y.

[49] M. Sangrà, J. Estelrich, R. Sabaté, A. Espargaró, and M. A. Busquets, 'Evidence of protein adsorption in pegylated liposomes: Influence of liposomal decoration', *Nanomaterials*, vol. 7, no. 2, Feb. 2017, doi: 10.3390/nano7020037.

[50] M. Mohamed *et al.*, 'PEGylated liposomes: immunological responses', *Sci Technol Adv Mater*, vol. 20, no. 1, p. 710, Dec. 2019, doi: 10.1080/14686996.2019.1627174.

[51] T. Gronemann, 'Elucidating the molecular interaction of blood serum proteins with fusogenic lipid nanoparticles as an advance drug delivery system.', RWTH Aachen , 2021.

[52] V. Kayser, N. Chennamsetty, V. Voynov, B. Helk, and B. L. Trout, 'Tryptophan-tryptophan energy transfer and classification of tryptophan residues in proteins using a therapeutic monoclonal antibody as a model', *J Fluoresc*, vol. 21, no. 1, pp. 1–20, Jan. 2011, doi: 10.1007/s10895-010-0715-0.

[53] A. Csiszár, N. Hersch, S. Dieluweit, R. Biehl, R. Merkel, and B. Hoffmann, 'Novel fusogenic liposomes for fluorescent cell labeling and membrane modification', *Bioconjug Chem*, vol. 21, no. 3, pp. 537–543, Mar. 2010, doi: 10.1021/BC900470Y.

[54] Malvern Instruments Ltd., 'Size theory', *Zetasizer Nano User Manual*, vol. MAN0485, no. 11, p. 250, 2013, [Online]. Available: https://www.chem.uci.edu/~dmitryf/manuals/Fundamentals/DLS measurement principles.pdf%0Ahttps://www.chem.uci.edu/~dmitryf/manuals/Malvern Zetasizer ZS DLS user manual.pdf

[55] V. A. Hackley and J. D. Clogston, 'Measuring the Hydrodynamic Size of Nanoparticles', *Characterization of Nanoparticles Intended for Drug Delivery*, vol. 697, no. 3, pp. 35–52, 2011, doi: 10.1007/978-1-60327-198-1.

[56] S. Bhattacharjee, 'DLS and zeta potential – What they are and what they are not?', *Journal of Controlled Release*, vol. 235, pp. 337–351, 2016, doi: https://doi.org/10.1016/j.jconrel.2016.06.017.

[57] R. Kolašinac, 'Characterization and application of fusogenic liposomes', Rheinische Friedrich-Wilhelms-Universität Bonn, 2020. Accessed: Jun. 12, 2022. [Online]. Available: https://bonndoc.ulb.uni-bonn.de/xmlui/handle/20.500.11811/8278

[58] J. R. Lakowicz, *Principles of fluorescence spectroscopy*. Springer, 2006.

[59] J. C. Croney, D. M. Jameson, and R. P. Learmonth, 'Fluorescence spectroscopy in biochemistry: teaching basic principles with visual demonstrations', *Biochemistry and Molecular Biology Education*, vol. 29, no. 2, pp. 60–65, 2001, doi: https://doi.org/10.1016/S1470-8175(01)00019-4.

[60] Y. Su, H. Ren, and X. Li, 'Novel nonequilibrium solvation theory for calculating the solvatochromic Stokes shift by State-specific TD-DFT', *Chem Phys Lett*, vol. 732, Oct. 2019, doi: 10.1016/J.CPLETT.2019.136640.

[61] Ottawa University, *1 - An Introduction to Fluorescence Spectroscopy User Assistance PerkinElmer Ltd Post Office Lane - StuDocu*. United Kingdom, 2014. Accessed: Jun. 12, 2022. [Online]. Available: https://www.studocu.com/en-us/document/ottawa-university/applications-of-spectroscopy-in-chemistry/1/2968783

[62] J. R. Lakowicz, *Principles of fluorescence spectroscopy*. Springer, 2006.

[63] V. D. Suryawanshi, L. S. Walekar, A. H. Gore, P. v. Anbhule, and G. B. Kolekar, 'Spectroscopic analysis on the binding interaction of biologically active pyrimidine derivative with bovine serum albumin', *J Pharm Anal*, vol. 6, no. 1, pp. 56–63, Feb. 2016, doi: 10.1016/J.JPHA.2015.07.001.

[64] M. Y. Arfat, Z. Arif, S. K. Chaturvedi, Moinuddin, and K. Alam, 'Peroxynitrite-induced structural perturbations in human IgG: A physicochemical study', *Arch Biochem Biophys*, vol. 603, pp. 72–80, Aug. 2016, doi: 10.1016/j.abb.2016.05.011.

[65] V. K. Srivastava and R. Yadav, 'Isothermal titration calorimetry', in *Data Processing Handbook for Complex Biological Data Sources*, Elsevier, 2019, pp. 125–137. doi: 10.1016/B978-0-12-816548-5.00009-5.

[66] A. J. Situ, T. Schmidt, P. Mazumder, and T. S. Ulmer, 'Characterization of membrane protein interactions by isothermal titration calorimetry', *J Mol Biol*, vol. 426, no. 21, pp. 3670–3680, Oct. 2014, doi: 10.1016/j.jmb.2014.08.020.

[67] T. Abraham, R. N. A. H. Lewis, R. S. Hodges, and R. N. McElhaney, 'Isothermal titration calorimetry studies of the binding of a rationally designed analogue of the antimicrobial peptide gramicidin S to phospholipid bilayer membranes', *Biochemistry*, vol. 44, no. 6, pp. 2103–2112, Feb. 2005, doi: 10.1021/bi048077d.

[68] K. E. Hevener, R. Pesavento, J. H. Ren, H. Lee, K. Ratia, and M. E. Johnson, 'Hit-to-Lead: Hit Validation and Assessment', in *Methods in Enzymology*, Academic Press Inc., 2018, pp. 265–309. doi: 10.1016/bs.mie.2018.09.022.

[69] P. Gagnon, R. Nian, D. Leong, and A. Hoi, 'Transient conformational modification of immunoglobulin G during purification by protein A affinity chromatography', *J Chromatogr A*, vol. 1395, pp. 136–142, May 2015, doi: 10.1016/J.CHROMA.2015.03.080.

[70] N. Oku *et al.*, 'Effect of serum protein binding on real-time trafficking of liposomes with different charges analyzed by positron emission tomography', 1996.

[71] O. A. Chaves *et al.*, 'Fluorescence and Docking Studies of the Interaction between Human Serum Albumin and Pheophytin', *Molecules*, vol. 20, no. 10, pp. 19526–19539, Oct. 2015, doi: 10.3390/MOLECULES201019526.

[72] V. Anbazhagan, R. S. Sankhala, B. P. Singh, and M. J. Swamy, 'Isothermal Titration Calorimetric Studies on the Interaction of the Major Bovine Seminal Plasma Protein, PDC-109 with Phospholipid Membranes', *PLoS One*, vol. 6, no. 10, p. 25993, 2011, doi: 10.1371/JOURNAL.PONE.0025993.

[73] M. S. Lin *et al.*, 'Kinetics and enthalpy measurements of interaction between beta-amyloid and liposomes by surface plasmon resonance and isothermal titration microcalorimetry', *Colloids Surf B Biointerfaces*, vol. 58, no. 2, pp. 231–236, Aug. 2007, doi: 10.1016/J.COLSURFB.2007.03.014.

[74] E. W. Becker, 'Dynamics and kinetics of enzymes. Kinetic equilibrium of forces in biochemistry', *Z Naturforsch C J Biosci*, vol. 47, no. 7–8, pp. 628–633, 1992, doi: 10.1515/ZNC-1992-7-823.

[75] T. Abraham, R. N. A. H. Lewis, R. S. Hodges, and R. N. McElhaney, 'Isothermal titration calorimetry studies of the binding of a rationally designed analogue of the antimicrobial peptide gramicidin s to phospholipid bilayer membranes', *Biochemistry*, vol. 44, no. 6, pp. 2103–2112, Feb. 2005, doi: 10.1021/BI048077D.

Appendix

Table A.1: The size and zeta measurement of FL in PBS and IgG, for the three individuals at 37 °C, pH: 7.40.

NPs	Size measurements						Zeta potential measurements			
	PBS			IgG			PBS		IgG	
	PK (nm)	PDI	Att.	PK (nm)	PDI	Att.	Zeta pot. (mV)	Att.	Zeta pot. (mV)	Att.
FL	342	0.2	8	955	1	8	25	9	-0.3	8
	396	0.2	7	1106	1	8	30	9	-0.7	9
	396	0.2	7	1106	0.8	8	29	10	-0.6	9

*PK: Peak position
*Att. Attenuator used in the measurement

Table A.2: The Size and zeta measurement of DOPC in PBS and IgG, for the three individuals.

NPs	Size measurements						Zeta potential measurements			
	PBS			IgG			PBS		IgG	
	PK (nm)	PDI	Att.	PK (nm)	PDI	Att.	Zeta pot. (mV)	Att.	Zeta pot. (mV)	Att.
DOPC	142	0.2	6	142	0.3	8	-8	10	-2	11
	164	0.3	7	164	0.5	8	-2	10	-1	11
	164	0.2	6	164	0.2	6	-7	9	-1	10

*PK: Peak position
*Att. Attenuator used in the measurement

Table A.3: The size and zeta measurement of DOPC-PEG in PBS and IgG, for the three individuals.

NPs	Size measurements						Zeta potential measurements			
	PBS			IgG			PBS		IgG	
	PK (nm)	PDI	Att.	PK (nm)	PDI	Att.	Zeta pot. (mV)	Att.	Zeta pot. (mV)	Att.
DOPC -PEG	106	0.1	7	106	0.3	8	-4	11	-6	10
	122	0.1	7	122	0.3	7	-9	10	-1	11
	122	0.1	8	122	0.3	8	-3	11	-14	10

*PK: Peak position
*Att. Attenuator used in the measurement

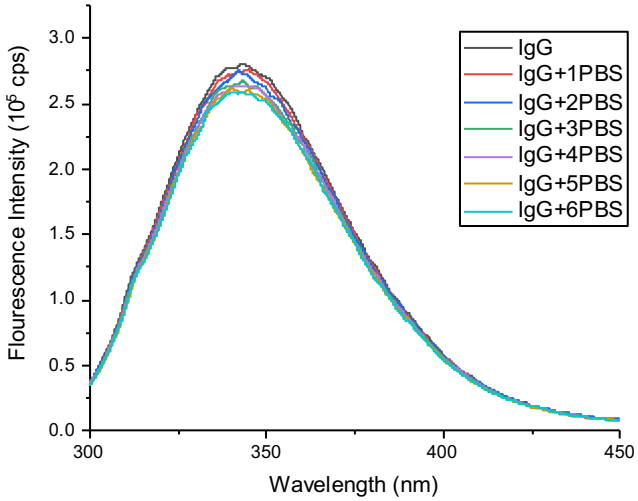

Figure A.1: Fluorescence emission spectra of the IgG dilution in buffer solution (pH=7.40, T=310K, $\lambda_{ex} = 283\ nm$). The black line refers to the emission spectrum of 0.5 μM free IgG. While the numbers of PBS added to IgG correspond to the emission spectrum after consecutive additions of $4\mu l\ of\ PBS$ (injection numbers, See (**Figure 3.9**)).

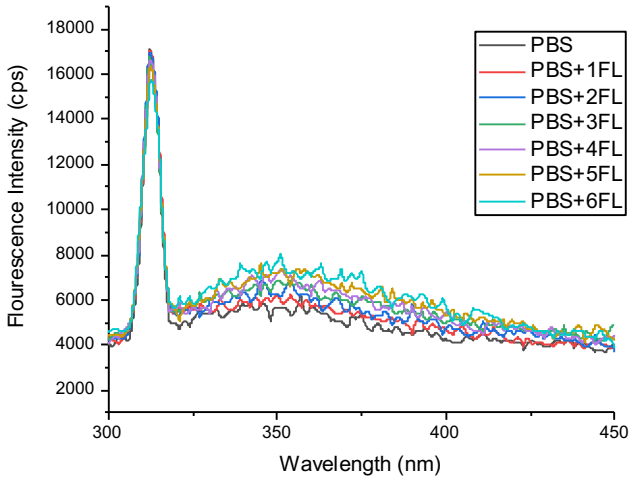

Figure A.2: Fluorescence emission spectra of FL dilution in buffer solution (pH=7.40, T=310K, $\lambda_{ex} = 283\ nm$). The black line refers to the emission spectrum of PBS. while the numbers of FL added to PBS correspond to the emission spectrum after consecutive additions of 4μl 5.2 μM FL (injection numbers, concentration range from 5.2 μM to 31 μM). See (**Figure 3.9**). The first peak here corresponds to Raman scattering of water.

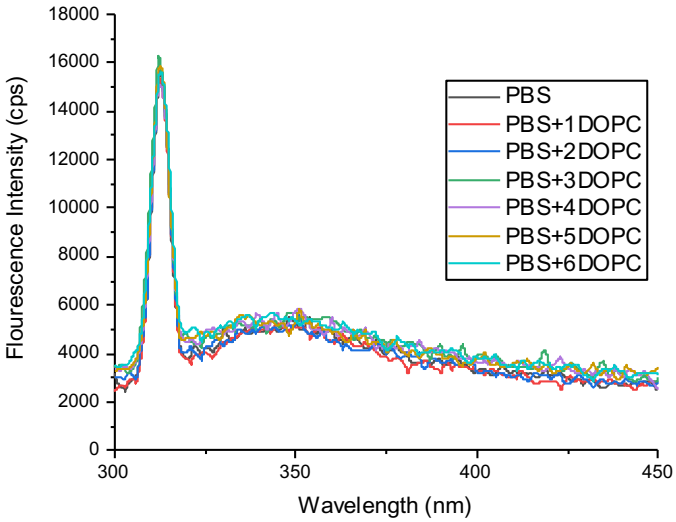

Figure A.3: Fluorescence emission spectra of DOPC dilution in buffer solution (pH=7.40, T=310K, $\lambda_{ex} = 283\ nm$). The black line refers to the emission spectrum of PBS. While the numbers of DOPC added to IgG correspond to the emission spectrum after consecutive additions of 4μl 4.2 μM DOPC (injection numbers, concentration range from 5.1 μM to 30.6 μM). See (**Figure 3.9**). The first peak here corresponds to Raman scattering of water.

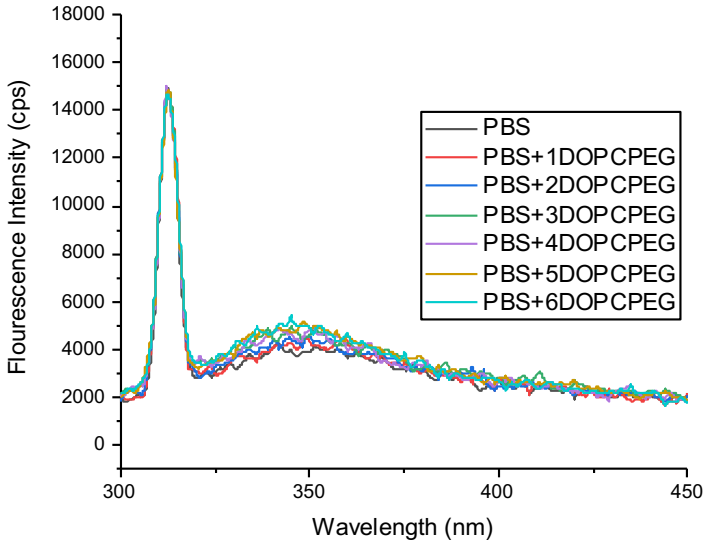

Figure A.4: Fluorescence emission spectra of DOPC-PEG dilution in buffer solution (pH=7.40, T=310K, $\lambda_{ex} = 283\ nm$). The black line refers to the emission spectrum of PBS. While the numbers of DOPC-PEG added to IgG correspond to the emission spectrum after consecutive additions of 4μl 4.2 μM DOPC-PEG (injection numbers, concentration range from 5.1 μM to 25.2 μM). See (**Figure 3.9**). The first peak here correspond to Raman scattering of water.